Superconductivity and spin-density waves in multiband metals

A. B. Vorontsov,[1] M. G. Vavilov,[2] and A. V. Chubukov[2]
[1]*Department of Physics, Montana State University, Bozeman, Montana 59717, USA*
[2]*Department of Physics, University of Wisconsin, Madison, Wisconsin 53706, USA*
(Received 11 March 2010; revised manuscript received 20 April 2010; published 28 May 2010)

We present a detailed description of two-band quasi-two-dimensional metals with *s*-wave superconducting (SC) and antiferromagnetic spin-density-wave (SDW) correlations. We present a general approach and use it to investigate the influence of the difference between the shapes and the areas of the two Fermi surfaces on the phase diagram. In particular, we determine the conditions for the coexistence of SC and SDW orders at different temperatures and dopings. We argue that a conventional *s*-wave SC order coexists with SDW order only at very low T and in a very tiny range of parameters. An extended *s*-wave superconductivity, for which SC gap changes sign between the two bands, coexists with antiferromagnetic SDW over a much wider range of parameters and temperatures but even for this SC order the regions of SDW and SC can still be separated by a first-order transition. We show that the coexistence range becomes larger if SDW order is incommensurate. We apply our results to iron-based pnictide materials, in some of which coexistence of SDW and SC orders has been detected.

DOI: 10.1103/PhysRevB.81.174538 PACS number(s): 74.25.Dw, 74.25.Ha

I. INTRODUCTION

Discovery of new magnetically active superconductors, iron pnictides, based on FeAs (Refs. 1 and 2) or Fe(Se,S,Te) (Refs. 3 and 4) has further invigorated the on-going discussions about coexistence of different ordered electronic states in metals.[5–7] In itinerant electrons systems, the interactions that lead to formation of superconducting (SC) and magnetic spin-density-wave (SDW) orders, "pull" and "push" the same particles, and as a result, influence each other. In particular, two orders may support each other and lead to homogeneous local coexistence of SC and SDW states; or one of them may completely suppress the other order, resulting in a state with spatially separated regions of "pure" SDW or SC orders. The transitions between various states may also be either continuous (second order) or abrupt (first order). The outcome of this interplay depends critically on a number of parameters: properties of the interactions, such as symmetry of SC pairing, their relative strengths, and also on properties the Fermi surface (FS), such as its shape or the density of electronic states.

In pnictides this parameter space is vast. First, these are multiband materials, with two hole pockets in the center, (0,0), and two electron pockets near $(\pm\pi,0)$ and $(0,\pm\pi)$ points of the unfolded Brillouin zone (BZ) (one Fe atom per unit cell). The shapes of quasi-two-dimensional electron pockets are quite distinct in different materials, ranging from simple circle-like types in LaOFeP,[8,9] to cross-like electronic FS in LaOFeAs,[9] to ellipses in $BaFe_2As_2$ (Refs. 10 and 11) and even more complex propeller-like structures in $(Ba,K)Fe_2As_2$ (Ref. 12) (for a descending point of view on this see Ref. 11). Hole pockets are near circular but different hole pockets in the same material usually have different sizes.

Second, multiple FSs also create a number of different possibilities[13,14] for electron ordering in the form of SDW, charge-density-wave states, and various superconducting states. The SC states include (1) the conventional s^{++}-wave state that has *s*-wave symmetry in the BZ and gaps of the same sign on electron and hole FSs; (2) the extended s^{+-} state that looks as *s* wave from a symmetry point of view but has opposite signs of the gaps on pockets at (0,0) and $(\pm\pi,0)$,[15–18] and (3) several SC states with the nodes in the SC gap, of both *s*-wave and *d*-wave symmetries.[19–23]

As a result of this complex environment, the interplay of magnetic and superconducting orders also shows some degree of variations. Most of parent compounds of iron pnictides are magnetically ordered. Upon doping, magnetism eventually yields to superconductivity but how this transformation occurs varies significantly between different Fe pnictides. A first-order transition between SC and SDW orders has been reported for $(La,Sm)O_{1-x}F_xFeAs$.[24,25] On the other hand, in electron-doped $Ba(Fe_{1-x}Co_x)_2As_2$ recent nuclear magnetic resonance,[26,27] specific heat, susceptibility, Hall coefficient,[2,28] and neutron-scattering experiments[29] indicate that SDW and SC phases coexist locally over some doping range. In the same 122 family, experiments on hole-doped $Ba_{1-x}K_x(FeAs)_2$ disagree with each other and indicate both coexistence[30,31] and incompatibility[27,32,33] of two orders. Isovalently doped 122 material $BaFe_2(As_{1-x}P_x)_2$ shows the region of coexistence.[34–36]

The goal of the present work is to understand how the system evolves from an SDW antiferromagnet to an s^{++}/s^{+-}-wave superconductor and how this evolution depends on the shape of the FS, the strengths of the interactions, and the structure of the SC order. For this we derive and solve a set of coupled nonlinear BCS-type equations for SC and SDW order parameters and compare values of the free energy for possible phases.

We report several results. First, we find that there is much more inclination for coexistence between s^{+-} and SDW orders than between the same-sign s^{++}-wave state and SDW. In the latter case, coexistence is only possible at very low T and in a very tiny range of parameters. Second, the coexistence region generally grows with increased strength of SDW coupling relative to superconducting interaction. That the coexistence is only possible when SDW transition comes first has been noticed some time ago[37,38] and our results agree with these findings. Third, when SDW order is commensurate, the coexistence is only possible when the following two condi-

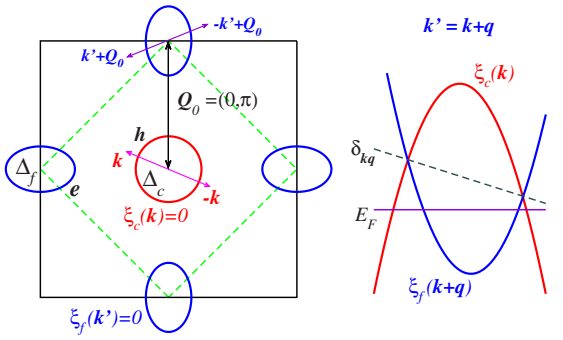

FIG. 1. (Color online) Left: electronic structure of the two-band model considered in this paper, in the unfolded Brillouin zone. The hole FS is in the center, with SC order parameter Δ_c, and the electron FSs are at $(0,\pi)$ and $(\pi,0)$, with SC order parameter Δ_f. The magnetic order with momentum $\mathbf{Q}_0=(0,\pi)$ hybridize hole and electron FSs separated by $\mathbf{Q}_0$ but leaves FSs at $(\pm\pi,0)$ intact. Right: by doping or pressure one may adjust the size and shape of hole and electron bands, and also SDW order parameter can be incommensurate, with momentum $\mathbf{Q}_0+\mathbf{q}$. These effects are described by FS detuning parameter, $\delta_{\mathbf{kq}}=[\xi_f(\mathbf{k}+\mathbf{q})+\xi_c(\mathbf{k})]/2$.

tions are met simultaneously: hole and electron FSs have different k_F (cross-section areas) *and* different shapes (e.g., hole pockets are circles and electron pockets are ellipses). Even then, SDW and SC orders coexist only in a limited range of parameters and temperatures, see Secs. IV and V, Figs. 10 and 15 below. When SDW order is incommensurate, the difference in k_F is a sufficient condition, but again, the two orders coexist in a limited range of parameters/temperatures (Fig. 11).

We also analyze in some detail the interplay between the coexistence and the presence of the Fermi surface (i.e., gapless excitations) in the SDW state. The "conventional" logic states that superconductivity and magnetism compete for the Fermi surface and coexist if SDW order still leaves a modified Fermi surface on which SC order can form. We find that the situation is more complex and the mere presence of absence of a modified Fermi surface is not the key reason for coexistence. We show that a more important reason is the effective "attraction" between SDW and SC order parameters, when the development of one order favors a gradual formation of the other order. Specifically, we show the following:

(a) Near the point where the transitions from the normal (N) state into SC and SDW states cross, SC can develop either via the coexistence phase or via a direct first-order transition between pure SDW and SC states. In this range, the SDW order parameter is small and SDW state is definitely a metal, Fig. 15.

(b) At low T, the coexistence phase may develop even when SDW state has no Fermi surface (not counting bands which do not participate in SDW). In this situation there is no Fermi surface for a conventional development of the SC order but the system still can lower the energy by developing both orders, if there is an attraction between them. This is the case for s^{+-} superconductivity and comparable strength of SDW and SC couplings, Figs. 7 and 10(a).

(c) The SDW phase at low T can be a metal with rather large Fermi surfaces, yet SC order does not develop. This is the case when SC order is s^{++}, Fig. 14.

The close connection between the coexistence of the two states and the symmetry of the SC state has been discussed earlier in the context of single-band heavy-fermion materials.[39] This connection gives a possibility to obtain information about the pure states (e.g., about the structure of the SC gap) from experimental investigations of the SC-SDW interplay, as it has been recently suggested.[29,40]

The structure of the paper is as follows. In the next section we define the model and derive generic equations for the SDW and SC order parameters and an expression for the free energy. Then we simplify these formulas for the case of a small splitting between hole and electron FSs and utilize them in Secs. III–V. In Sec. III we focus on a pure SDW state, with special attention given to the interplay between ellipticity of the FS and the incommensuration of the SDW order. In the next two sections we discuss possible coexistence of SDW and SC states: in Sec. IV we present numerical results obtained in a wide range of temperatures and dopings, and in Sec. V we corroborate this with the analytical consideration in the vicinity of the crossing point of SC and SDW transitions, and at $T=0$. In Sec. VI we model the case when the splitting between the two FSs is not small. We present our conclusions in Sec. VII. Some of the results reported in this work have been presented in shorter publications.[41,42]

II. MODEL AND ANALYTICAL REASONING

A. General formulation

Since the basic properties of the SC and magnetic SDW interactions and their interplay should not depend on the number of bands significantly, we consider a basic model of one hole and one-electron bands. For pnictides this means that we neglect the double degeneracy of hole and electron states at the center and the corners of the Brillouin zone, which does not seem to be essential for superconducting[20,22,23,43–46] or magnetic order.[47–51]

The basic model is illustrated in Fig. 1. Electronic structure contains two families of fermions, near one-hole and one-electron FSs of small and near-equal sizes. Such two-band structure yields the experimentally observed stripe $(\pi,0)$ or $(0,\pi)$ magnetic order which in itinerant scenario appears, at least partly, due to nesting between one-hole and one-electron bands, separated by momentum $(\pi,0)$ or $(0,\pi)$. Other hole and electron bands do not participate in the SDW order. We assume that SC also primarily resides on the same two FSs, at least close to the boundary of the SDW phase. The SC order parameter on the other two bands is not zero but is smaller. Once doping increases and the system moves away from SDW boundary, we expect that the magnitudes of the SC order parameter on the two electron bands should become closer to each other.

The basic Hamiltonian includes the free fermion part $\mathcal{H}_0$, and the fermion-fermion interactions in superconducting and magnetic SDW channels,

$$\mathcal{H}=\mathcal{H}_0+\mathcal{H}_\Delta+\mathcal{H}_m. \tag{2.1}$$

The free fermion part of the Hamiltonian is

$$\mathcal{H}_0 = \sum_{\mathbf{k}} \xi_c(\mathbf{k}) c^\dagger_{\mathbf{k}\alpha} c_{\mathbf{k}\alpha} + \sum_{\mathbf{k}'} \xi_f(\mathbf{k}') f^\dagger_{\mathbf{k}'\alpha} f_{\mathbf{k}'\alpha}, \tag{2.2}$$

where creation/annihilation $c^\dagger$, c operators correspond to fermions near the central hole pocket (0,0), and f operators describe fermions near the electron pocket at $\mathbf{Q}_0=(0,\pi)$ and the fermion dispersions near the pockets are

$$\xi_c(\mathbf{k}) = \mu_c - \frac{\mathbf{k}^2}{2m_c}, \quad \xi_f(\mathbf{k}) = \frac{k_x^2}{2m_{fx}} + \frac{k_y^2}{2m_{fy}} - \mu_f. \tag{2.3}$$

The momenta $\mathbf{k}$ are measured from the center of the BZ and $\mathbf{k}'$ are deviations from $\mathbf{Q}_0$. We assume an inversion symmetry, $\xi_{c,f}(-\mathbf{k})=\xi_{c,f}(\mathbf{k})$.

The pairing interaction consists of many different pair scattering terms but the most important one is the pair hopping between the hole and electron pockets,[13,22]

$$\mathcal{H}_\Delta = \frac{1}{2}\sum_{\mathbf{k},\mathbf{p}} V^{cf}_{\alpha\beta\beta'\alpha'}(\mathbf{k},\mathbf{p})(c^\dagger_{\mathbf{k}\alpha} c^\dagger_{-\mathbf{k}\beta} f_{-\mathbf{p}\beta'} f_{\mathbf{p}\alpha'} + f^\dagger_{\mathbf{k}\alpha} f^\dagger_{-\mathbf{k}\beta} c_{-\mathbf{p}\beta'} c_{\mathbf{p}\alpha'}). \tag{2.4}$$

For definiteness, we consider SC interaction only in the singlet channel, i.e.,

$$V^{cf}_{\alpha\beta\beta'\alpha'}(\mathbf{k},\mathbf{p}) = V^{SC}_{\mathbf{k},\mathbf{p}} (i\sigma^y)_{\alpha\beta} (i\sigma^y)^\dagger_{\beta'\alpha'}. \tag{2.5}$$

The magnetic interaction between fermions is

$$\mathcal{H}_m = -\frac{1}{4}\sum_{\mathbf{p}'-\mathbf{p}=\mathbf{k}'-\mathbf{k}} V^{SDW}_{\alpha\beta\beta'\alpha'}(\mathbf{p}'\mathbf{p};\mathbf{k},\mathbf{k}')(f^\dagger_{\mathbf{p}'\alpha} c_{\mathbf{p}\beta} c^\dagger_{\mathbf{k}\beta'} f_{\mathbf{k}'\alpha'} + f^\dagger_{-\mathbf{p}'\alpha} c_{-\mathbf{p}\beta} c^\dagger_{-\mathbf{k}\beta'} f_{-\mathbf{k}'\alpha'}), \tag{2.6}$$

where we symmetrized the expression with respect to particle hopping between $(0,0)-(0,\pi)$ and $(0,0)-(0,-\pi)$ pockets for later convenience. We take the interaction matrix in a simple form

$$V^{SDW}_{\alpha\beta\beta'\alpha'}(\mathbf{p}'\mathbf{p};\mathbf{k}\mathbf{k}') = V^{SDW}_{\mathbf{p}'\mathbf{p};\mathbf{k}\mathbf{k}'} \boldsymbol{\sigma}_{\alpha\beta}\cdot\boldsymbol{\sigma}^\dagger_{\beta'\alpha'} \tag{2.7}$$

with a constant $V^{SDW}_{\mathbf{p}'\mathbf{p};\mathbf{k}\mathbf{k}'}=V^{SDW}$.

The evolution of the interaction couplings with energy was considered in Ref. 13. Here we assume that the interactions for low-energy excitations can be represented in terms of fermion couplings to order-parameter fields in the SC and SDW channels. In the spirit of BCS-type approach, we introduce the SC order parameters

$$\Delta_c(\mathbf{k})_{\alpha\beta} = (i\sigma^y)_{\alpha\beta}\sum_{\mathbf{p}} V^{SC}_{\mathbf{k},\mathbf{p}} (i\sigma^y)^\dagger_{\beta'\alpha'} \langle f_{-\mathbf{p}\beta'} f_{\mathbf{p}\alpha'}\rangle, \tag{2.8a}$$

$$\Delta_f(\mathbf{k})_{\alpha\beta} = (i\sigma^y)_{\alpha\beta}\sum_{\mathbf{p}} V^{SC}_{\mathbf{k},\mathbf{p}} (i\sigma^y)^\dagger_{\beta'\alpha'} \langle c_{-\mathbf{p}\beta'} c_{\mathbf{p}\alpha'}\rangle, \tag{2.8b}$$

and the SDW order parameter directed along $\hat{\mathbf{m}}$. We assume that SDW order parameter has a single ordering momentum $\mathbf{Q}=\mathbf{Q}_0+\mathbf{q}$ in which case it is fully specified by $(m_\mathbf{q})_{\alpha\beta} = (\mathbf{m}_\mathbf{q}\boldsymbol{\sigma})_{\alpha\beta} = m_\mathbf{q}(\hat{\mathbf{m}}\boldsymbol{\sigma})_{\alpha\beta}$, where

$$(m_\mathbf{q})_{\alpha\beta} = -V^{SDW}\frac{1}{2}\sum_{\mathbf{p}} \boldsymbol{\sigma}_{\alpha\beta}\cdot\boldsymbol{\sigma}^\dagger_{\beta'\alpha'} \langle c^\dagger_{\mathbf{p}\beta'} f_{\mathbf{p}+\mathbf{q}\alpha'}\rangle = -V^{SDW}\frac{1}{2}\sum_{\mathbf{p}} \boldsymbol{\sigma}_{\alpha\beta}\cdot\boldsymbol{\sigma}^\dagger_{\beta'\alpha'} \langle f^\dagger_{-\mathbf{p}-\mathbf{q}\beta'} c_{-\mathbf{p}\alpha'}\rangle. \tag{2.8c}$$

Since $\langle c^\dagger_{\mathbf{p}\alpha} f_{\mathbf{p}+\mathbf{q}\beta}\rangle \sim (\mathbf{m}_\mathbf{q}\boldsymbol{\sigma})_{\alpha\beta}$, the corresponding electronic magnetization,

$$\mathbf{m}(\mathbf{R}) = \sum_{\mathbf{p}} \boldsymbol{\sigma}_{\alpha\beta}[\langle c^\dagger_{\mathbf{p}\alpha} f_{\mathbf{p}+\mathbf{q}\beta}\rangle e^{i\mathbf{Q}\mathbf{R}} + \langle f^\dagger_{\mathbf{p}+\mathbf{q}\alpha} c_{\mathbf{p}\beta}\rangle e^{-i\mathbf{Q}\mathbf{R}}]$$

is $\mathbf{m}_\mathbf{q}\cos\mathbf{Q}\mathbf{R}$ for real $\mathbf{m}_\mathbf{q}$ and is $\mathbf{m}'_\mathbf{q}\cos\mathbf{Q}\mathbf{R} - \mathbf{m}''_\mathbf{q}\sin\mathbf{Q}\mathbf{R}$ for a complex $\mathbf{m}_\mathbf{q}=\mathbf{m}'_\mathbf{q}+i\mathbf{m}''_\mathbf{q}$. In principle, SDW order parameter may contain several components with different $\mathbf{q}$, which could give rise to domainlike structures of $\mathbf{m}(\mathbf{R})$. For recent studies in this direction see Ref. 52. We perform the analysis of the coexistence between SC order and SDW order with a single $\mathbf{q}$. A more general form of the SDW order should not qualitatively change the phase diagram for SC and SDW states, however this assumption requires further verifications.

Using the forms of SC and SDW order parameters, we write the free and interaction parts in quadratic forms as

$$\mathcal{H}_0 = \frac{1}{2}\sum_{\mathbf{k}} [\xi_c(\mathbf{k}) c^\dagger_{\mathbf{k}\alpha} c_{\mathbf{k}\alpha} + \xi_c(-\mathbf{k}) c^\dagger_{-\mathbf{k}\alpha} c_{-\mathbf{k}\alpha} + \xi_f(\mathbf{k}+\mathbf{q}) f^\dagger_{\mathbf{k}+\mathbf{q}\alpha} f_{\mathbf{k}+\mathbf{q}\alpha} + \xi_f(-\mathbf{k}-\mathbf{q}) f^\dagger_{-\mathbf{k}-\mathbf{q}\alpha} f_{-\mathbf{k}-\mathbf{q}\alpha}], \tag{2.9}$$

$$\mathcal{H}_\Delta = \frac{1}{2}\sum_{\mathbf{k}} [\Delta_c(\mathbf{k})_{\alpha\beta} c^\dagger_{\mathbf{k}\alpha} c^\dagger_{-\mathbf{k}\beta} + \Delta^\dagger_c(\mathbf{k})_{\alpha\beta} c_{-\mathbf{k}\alpha} c_{\mathbf{k}\beta} + \Delta_f(\mathbf{k}+\mathbf{q})_{\alpha\beta} f^\dagger_{\mathbf{k}+\mathbf{q}\alpha} f^\dagger_{-\mathbf{k}-\mathbf{q}\beta} + \Delta^\dagger_f(\mathbf{k}+\mathbf{q})_{\alpha\beta} f_{-\mathbf{k}-\mathbf{q}\alpha} f_{\mathbf{k}+\mathbf{q}\beta}], \tag{2.10}$$

$$\mathcal{H}_m = \frac{1}{2}\sum_{\mathbf{k}} [m_{\mathbf{q},\alpha\beta} f^\dagger_{\mathbf{k}+\mathbf{q}\alpha} c_{\mathbf{k}\beta} + m_{\mathbf{q},\alpha\beta} c^\dagger_{-\mathbf{k}\alpha} f_{-\mathbf{k}-\mathbf{q}\beta} + m^\dagger_{\mathbf{q},\alpha\beta} c^\dagger_{\mathbf{k}\alpha} f_{\mathbf{k}+\mathbf{q}\beta} + m^\dagger_{\mathbf{q},\alpha\beta} f^\dagger_{-\mathbf{k}-\mathbf{q}\alpha} c_{-\mathbf{k}\beta}]. \tag{2.11}$$

Hamiltonian Eq. (2.1) can be represented in the matrix form

$$\mathcal{H} = \frac{1}{2}\sum_{\mathbf{k}\alpha\beta} \bar{\Psi}_{\mathbf{k}\alpha} \hat{\mathcal{H}}_\mathbf{k} \Psi_{\mathbf{k}\beta}, \qquad \hat{\mathcal{H}}_\mathbf{k} = \left(\begin{array}{cc|cc} \xi_c(\mathbf{k}) & \Delta_c(\mathbf{k}) i\sigma^y_{\alpha\beta} & m^*_\mathbf{q}(\hat{\mathbf{m}}\boldsymbol{\sigma})^\dagger_{\alpha\beta} & 0 \\ -\Delta^*_c(\mathbf{k}) i\sigma^y_{\alpha\beta} & -\xi_c(-\mathbf{k}) & 0 & -m^*_\mathbf{q}(\hat{\mathbf{m}}\boldsymbol{\sigma}^{\mathrm{T}})^\dagger_{\alpha\beta} \\ \hline m_\mathbf{q}(\hat{\mathbf{m}}\boldsymbol{\sigma})_{\alpha\beta} & 0 & \xi_f(\mathbf{k}+\mathbf{q}) & \Delta_f(\mathbf{k}+\mathbf{q}) i\sigma^y_{\alpha\beta} \\ 0 & -m_\mathbf{q}(\hat{\mathbf{m}}\boldsymbol{\sigma}^{\mathrm{T}})_{\alpha\beta} & -\Delta^*_f(\mathbf{k}+\mathbf{q}) i\sigma^y_{\alpha\beta} & -\xi_f(-\mathbf{k}-\mathbf{q}) \end{array}\right), \tag{2.12}$$

with $\bar{\Psi}_{\mathbf{k}\alpha}=(c^{\dagger}_{\mathbf{k}\alpha}, c_{-\mathbf{k}\alpha}, f^{\dagger}_{\mathbf{k}+\mathbf{q}\alpha}, f_{-\mathbf{k}-\mathbf{q}\alpha})$ and Ψ being its conjugated column. The two diagonal blocks of the matrix $\hat{\mathcal{H}}_{\mathbf{k}}$ correspond to a purely SC system with Δ_c and Δ_f living on two different bands, and two off-diagonal blocks contain SDW field $m_{\mathbf{q}}$ that couples fermions between the two bands.

To solve this system of equations for the SC and SDW order parameters, Eq. (2.7), we define the imaginary-time Green's function

$$\hat{G}(\mathbf{k},\tau)_{\alpha\beta}=-\langle T_\tau \Psi(\tau)_{\mathbf{k}\alpha}\bar{\Psi}(0)_{\mathbf{k}\beta}\rangle \equiv \begin{pmatrix} \hat{G}_{cc} & \hat{G}_{cf} \\ \hat{G}_{fc} & \hat{G}_{ff} \end{pmatrix}, \tag{2.13}$$

which satisfies the Dyson equation,

$$\hat{G}^{-1}(\mathbf{k},\varepsilon_n)=i\varepsilon_n-\hat{\mathcal{H}}_{\mathbf{k}}, \tag{2.14}$$

where $\varepsilon_n=\pi T(2n+1)$ are the Matsubara frequencies. The system of equations is closed by the self-consistency equations for the SC and SDW order parameters in terms of this Green's function,

$$\Delta_c(\mathbf{k})=\sum_{\mathbf{p}} V^{SC}_{\mathbf{k},\mathbf{p}} T\sum_{\varepsilon_n} \mathrm{Tr}\{(i\sigma^y)^{\dagger}\hat{\tau}_+\hat{G}_{ff}(\mathbf{p},\varepsilon_n)\}, \tag{2.15}$$

$$\Delta_f(\mathbf{k})=\sum_{\mathbf{p}} V^{SC}_{\mathbf{k},\mathbf{p}} T\sum_{\varepsilon_n} \mathrm{Tr}\{(i\sigma^y)^{\dagger}\hat{\tau}_+\hat{G}_{cc}(\mathbf{p},\varepsilon_n)\}, \tag{2.16}$$

$$m_{\mathbf{q}}=-\sum_{\mathbf{p}} V^{SDW}\frac{T}{4}\sum_{\varepsilon_n} \mathrm{Tr}\{(\hat{\mathbf{m}}\boldsymbol{\sigma}_4)\hat{\tau}_3\hat{G}_{fc}(\mathbf{p},i\varepsilon_n)\}. \tag{2.17}$$

Henceforth we define Pauli matrices in particle-hole space, $\hat{\tau}_{1,2,3}$, $\hat{\tau}_{\pm}=(\hat{\tau}_1\pm\hat{\tau}_2)/2$, and the following matrices in spin- and particle-hole space,

$$\hat{\Delta}=\begin{pmatrix} 0 & (\Delta\ i\sigma^y)_{\alpha\beta} \\ (\Delta\ i\sigma^y)^{\dagger}_{\alpha\beta} & 0 \end{pmatrix}, \quad \boldsymbol{\sigma}_4=\begin{pmatrix} \boldsymbol{\sigma} & 0 \\ 0 & \boldsymbol{\sigma}^{\mathrm{T}} \end{pmatrix}. \tag{2.18}$$

The expressions above are valid for complex $\Delta(\mathbf{k})$ and $m_{\mathbf{q}}$. Below, to simplify formulas, we assume that Δ's and $m_{\mathbf{q}}$ are real, i.e., consider only "sinusoidal," cos**QR**, variations in the SDW order parameter. To lighten the notations, we will also drop the momenta arguments $(\mathbf{k},\mathbf{k}+\mathbf{q})$ in $\xi_{c,f}$, $\Delta_{c,f}$ and the subscript in $m_{\mathbf{q}}$ [still implying this dependence as it appears in Eq. (2.12)].

The equations for components of the Green's function are obtained from inversion of Eq. (2.14),

$$\hat{G}^{-1}_{cc}=\hat{G}^{-1}_{c0}-m^2\hat{G}_{f0}, \quad \hat{G}_{fc}=\hat{M}\hat{G}_{f0}\hat{G}_{cc}, \tag{2.19a}$$

$$\hat{G}^{-1}_{ff}=\hat{G}^{-1}_{f0}-m^2\hat{G}_{c0} \tag{2.19b}$$

with definition

$$\begin{pmatrix} \hat{G}^{-1}_{c0} & -\hat{M} \\ -\hat{M} & \hat{G}^{-1}_{f0} \end{pmatrix} \equiv \left(\begin{array}{c|c} i\varepsilon_n-\xi_c\hat{\tau}_3-\hat{\Delta}_c & -(\mathbf{m}\boldsymbol{\sigma}_4)\hat{\tau}_3 \\ \hline -(\mathbf{m}\boldsymbol{\sigma}_4)\hat{\tau}_3 & i\varepsilon_n-\xi_f\hat{\tau}_3-\hat{\Delta}_f \end{array}\right). \tag{2.20}$$

To obtain Eq. (2.19) we used the fact that the magnetic matrix $\hat{M}$ commutes with purely superconducting parts, $[\hat{M},\hat{G}_{c0}]=[\hat{M},\hat{G}_{f0}]=0$, and $\hat{M}\hat{M}=m^2$.

The diagonal Green's functions $\hat{G}_{c0}$ and $\hat{G}_{f0}$ are the same as in a pure superconductor, e.g.,

$$\hat{G}_{f0}(\varepsilon_n)=\frac{\hat{G}^{-1}_{f0}(-\varepsilon_n)}{D_{f0}}, \quad D_{f0}=\varepsilon_n^2+\xi_f^2+\Delta_f^2, \tag{2.21}$$

where for inversion we used the relations

$$\{\hat{\tau}_3,\hat{\Delta}\}=0, \quad [(\hat{\mathbf{m}}\boldsymbol{\sigma}_4)\hat{\tau}_3,\hat{\Delta}]=0, \quad \hat{\Delta}^2=\Delta^2, \tag{2.22}$$

which are also employed to invert 4×4 matrices for mixed SC+SDW state. For example, for $\hat{G}_{cc}$ we have

$$\hat{G}_{cc}(\varepsilon_n)=\frac{1}{\hat{G}^{-1}_{c0}(\varepsilon_n)-m^2\hat{G}^{-1}_{f0}(-\varepsilon_n)/D_{f0}}, \tag{2.23}$$

and with the above relations in mind it becomes

$$\hat{G}_{cc}=\hat{G}^{(1)}_{cc}+\hat{G}^{(\tau_3)}_{cc}+\hat{G}^{(\Delta)}_{cc}, \tag{2.24a}$$

where

$$\hat{G}^{(1)}_{cc}=\frac{-i\varepsilon_n(D_{f0}+m^2)}{D}, \tag{2.24b}$$

$$\hat{G}^{(\tau_3)}_{cc}=-\frac{\xi_c D_{f0}-\xi_f m^2}{D}\hat{\tau}_3, \tag{2.24c}$$

$$\hat{G}^{(\Delta)}_{cc}=-\frac{\hat{\Delta}_c D_{f0}-\hat{\Delta}_f m^2}{D}. \tag{2.24d}$$

The denominator

$$D=\frac{\varepsilon_n^2(D_{f0}+m^2)^2+(\xi_c D_{f0}-\xi_f m^2)^2+(\Delta_c D_{f0}-\Delta_f m^2)^2}{D_{f0}}$$

$$=(\varepsilon_n^2+\xi_c^2+\Delta_c^2)(\varepsilon_n^2+\xi_f^2+\Delta_f^2)+2m^2(\varepsilon_n^2-\xi_c\xi_f-\Delta_c\Delta_f)+m^4$$

$$=(\varepsilon_n^2+E_+^2)(\varepsilon_n^2+E_-^2) \tag{2.25}$$

gives the energies of new excitations in the system, cf. Ref. 29. We obtained (explicitly showing $\mathbf{k}$ and $\mathbf{q}$ here),

$$E^2_{\pm}=\xi^2_{\mathbf{kq}}+\delta^2_{\mathbf{kq}}+m^2+(\Delta^-_{\mathbf{kq}})^2 + (\Delta^+_{\mathbf{kq}})^2\pm 2\sqrt{m^2[(\Delta^+_{\mathbf{kq}})^2+\delta^2_{\mathbf{kq}}]+(\Delta^-_{\mathbf{kq}}\Delta^+_{\mathbf{kq}}+\xi_{\mathbf{kq}}\delta_{\mathbf{kq}})^2} \tag{2.26}$$

with

$$\xi_{\mathbf{kq}}=\frac{\xi_f(\mathbf{k}+\mathbf{q})-\xi_c(\mathbf{k})}{2}, \tag{2.27}$$

$$\delta_{\mathbf{kq}} = \frac{\xi_f(\mathbf{k}+\mathbf{q}) + \xi_c(\mathbf{k})}{2} \tag{2.28}$$

and

$$\Delta^-_{\mathbf{kq}} = \frac{\Delta_f(\mathbf{k}+\mathbf{q}) - \Delta_c(\mathbf{k})}{2}, \tag{2.29}$$

$$\Delta^+_{\mathbf{kq}} = \frac{\Delta_f(\mathbf{k}+\mathbf{q}) + \Delta_c(\mathbf{k})}{2}. \tag{2.30}$$

The parameter $\xi_{\mathbf{kq}}$ describes the dispersion and the parameter $\delta_{\mathbf{kq}}$ describes deviations of the electron and hole FSs from perfect nesting, as illustrated in Figs. 1 and 2. For the interband part of the Green's function we obtain

$$\hat{G}_{fc}(\varepsilon_n) = \hat{M}\hat{G}_{f0}\hat{G}_{cc}$$

$$= \hat{M}\hat{G}_{f0}(\varepsilon_n)\frac{\hat{G}^{-1}_{c0}(-\varepsilon_n)D_{f0} - m^2\hat{G}^{-1}_{f0}(\varepsilon_n)}{D}$$

$$= \hat{M}\frac{\hat{G}^{-1}_{f0}(-\varepsilon_n)\hat{G}^{-1}_{c0}(-\varepsilon_n) - m^2}{D}, \tag{2.31}$$

where for self-consistency Eq. (2.17) we need only the part proportional purely to $\hat{M}$-matrix, Eq. (2.20),

$$\hat{G}^{(M)}_{fc} = (\mathbf{m}\boldsymbol{\sigma}_4)\hat{\tau}_3\frac{-\varepsilon_n^2 + \xi_f\xi_c + \Delta_f\Delta_c - m^2}{D}. \tag{2.32}$$

Expressions for $\hat{G}_{ff}$ and $\hat{G}_{cf}$ are obtained from Eqs. (2.32) by swapping indices, $c \leftrightarrow f$.

We substitute the above expressions for $\hat{G}^{(\Delta)}_{cc}(\mathbf{p})$, $\hat{G}^{(\Delta)}_{ff}(\mathbf{p}+\mathbf{q})$, and $\hat{G}^{(M)}_{fc}(\mathbf{p})$ into the self-consistency equations Eqs. (2.15)–(2.17) and arrive at

$$\Delta_f(\mathbf{k}) = T\sum_{\varepsilon_n}\sum_{\mathbf{p}}(-2V^{SC}_{\mathbf{kp}})\frac{\Delta_c(\mathbf{p})[\varepsilon_n^2 + \xi_f^2(\mathbf{p}+\mathbf{q}) + \Delta_f^2(\mathbf{p}+\mathbf{q})] - \Delta_f(\mathbf{p}+\mathbf{q})m^2}{D}, \tag{2.33}$$

$$\Delta_c(\mathbf{k}) = T\sum_{\varepsilon_n}\sum_{\mathbf{p}}(-2V^{SC}_{\mathbf{kp+q}})\frac{\Delta_f(\mathbf{p}+\mathbf{q})[\varepsilon_n^2 + \xi_c^2(\mathbf{p}) + \Delta_c^2(\mathbf{p})] - \Delta_c(\mathbf{p})m^2}{D}, \tag{2.34}$$

$$m = T\sum_{\varepsilon_n}\sum_{\mathbf{p}}V^{SDW}\frac{\varepsilon_n^2 + m^2 - \xi_f(\mathbf{p}+\mathbf{q})\xi_c(\mathbf{p}) - \Delta_f(\mathbf{p}+\mathbf{q})\Delta_c(\mathbf{p})}{D}m. \tag{2.35}$$

To calculate the relative stability of different states, one also needs to evaluate the free energy. We follow the Luttinger-Ward[53] and De Dominicis-Martin[54] method, and consider the functional[55]

$$F = -\frac{1}{2}Sp\{\hat{\Sigma}\hat{G} + \ln[-(i\varepsilon_n - \hat{\xi}) + \hat{\Sigma}]\} + \Phi[\hat{G}], \tag{2.36}$$

which, if minimized with respect to $\hat{G}$, gives self-consistency equations, $\hat{\Sigma}[\hat{G}] = 2\delta\Phi[\hat{G}]/\delta\hat{G}$, and, if minimized with respect to $\hat{\Sigma}$, gives the Dyson equation, Eq. (2.14). Here Sp is the trace over two fermion bands, spin, particle-hole matrix structure, and the sum over Matsubara energies and the integral over momenta, and $\hat{\Sigma}$ is the mean-field SC and SDW order-parameter matrix,

$$\hat{\Sigma} = \begin{pmatrix} \hat{\Delta}_c & \hat{M} \\ \hat{M} & \hat{\Delta}_f \end{pmatrix}. \tag{2.37}$$

The functional $\Phi[\hat{G}]$ producing the self-consistency equations is a quadratic function of $\hat{G}$. Using the self-consistency equations one can explicitly verify that at weak coupling it can be written as $\Phi[\hat{G}] = \frac{1}{4}Sp\{\hat{\Sigma}\hat{G}\}$. To deal with the logarithm in Eq. (2.36) one introduces a continuous variable λ instead of ε_n, differentiates the logarithmic term with respect to λ to obtain the Green's function $\hat{G}(\lambda) = (i\lambda - \hat{\xi} - \hat{\Sigma})^{-1}$, and then integrates back to get the difference between a condensed state and the normal state for fixed external parameters, such as temperature or field,

$$\Delta F(\Delta_{c,f}, m) = -\frac{1}{2}Sp\left\{\frac{1}{2}\hat{\Sigma}\hat{G} - \int_{\varepsilon_n}^{\infty} d\lambda[i\hat{G}(\lambda) - i\hat{G}_N(\lambda)]\right\}, \tag{2.38}$$

where $\hat{G}_N$ is the Green's function in the normal state without either SC or SDW order and we used the fact that in the normal state $\hat{\Sigma} = 0$. Substituting into Eq. (2.38) the Green's functions Eqs. (2.32), the self-energy Eq. (2.37), and using the self-consistency equations Eqs. (2.33)–(2.35) to eliminate the high-energy cutoffs in order to regularize the ε_n summation and $\mathbf{k}$ integration, one obtains the most general free-energy functional for given $\Delta_{c,f}$ and m.

B. Limit of small Fermi-surface splitting

In principle, equations for full Green's functions Eq. (2.32), the self-consistency equations Eqs. (2.33)–(2.35) and the free energy Eq. (2.38), completely describe the system in

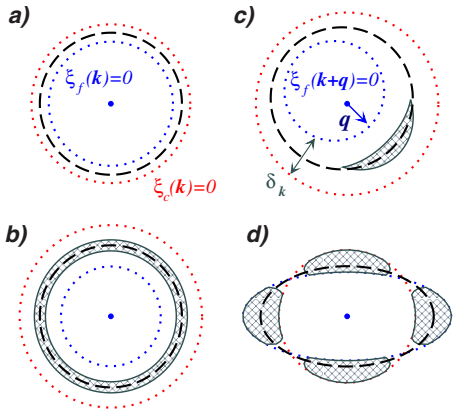

FIG. 2. (Color online) The appearance of gapless excitations in the presence of SDW order. The dotted lines indicate FSs for electrons, $\xi_f=0$, and holes, $\xi_c=0$. The dashed curve is an "effective" FS, $\xi_{\mathbf{kq}}=0$. (a) When $q=0$ and m is large compared to FS mismatch, $m>\delta_{\hat{\mathbf{k}}0}$, all excitations are gapped; (b) when m is small, gapless excitations are preserved along the two modified FSs at $\xi_{\mathbf{k},0}=\pm(\delta^2_{\hat{\mathbf{k}},0}-m^2)^{1/2}$ ($|\delta_{\hat{\mathbf{k}},0}|>m$ in the shaded region). Such gapless state, however, only exists at high temperatures while at low T it is pre-emptied by a first-order transition to the normal state (Ref. 42); (c) to prevent the first-order transition, magnetic order is formed at an incommensurate vector $\mathbf{Q}=\mathbf{Q}_0+\mathbf{q}$. This improves electron-hole nesting on some part of the FS but allows for gapless excitations at the opposite side; (d) when the two FSs are of different shapes, the nested parts become gapped due to SDW order and on the rest of the FSs the excitations are little affected by SDW order. The density of states for these cases is shown in Fig. 3.

a very general case. However, to proceed further with the analytics one can reduce the number of summations which is also desirable from a numerical standpoint.

The typical approximation is to linearize the dispersion near the FS and integrate out the momenta in the direction normal to the FS over $\xi_{\mathbf{kq}}$. In the case, when the two FSs are reasonably close to each other [when shifted by $(0,\pi)$], and electron and hole dispersions are similar, the values of FS mismatch $\delta_{\mathbf{kq}}$ are weakly momentum dependent, and can be taken at positions where $\xi_{\mathbf{kq}}=0$.

The consequence of this approximation, which we discuss in some detail in the Appendix, is that $\delta_{\mathbf{kq}}$ depends only on the angle in $\mathbf{k}$ space, but not on $\xi_{\mathbf{kq}}$ and hence one can integrate along a particular direction $\hat{\mathbf{k}}$ over $\xi_{\mathbf{kq}}$, keeping $\delta_{\hat{\mathbf{kq}}}$ fixed.

Within this approximation the density of states (DOS) for both FSs are the same, and the magnitudes of Δ_c and Δ_f are equal (the angular dependence of SC gaps is still determined by that of the SC interactions). There are, indeed, also higher order terms, which we neglected in the last lines of Eq. (A2). These terms make hole and electron DOS different from each other, what in turn makes $|\Delta_c|$ and $|\Delta_f|$ nonequal, but these terms are small in $\delta_{\mathbf{k}}/\mu_{c,f}$ and only account for subleading terms in the free energy, $\mu_{c,f}$ are Fermi energies of electron and hole bands, Eq. (2.3).

This approximation comes at certain price. When two FSs are of very different shapes, approximating them as small deviations from a single line in $\mathbf{k}$ space everywhere is incorrect. This is shown, for example, in Fig. 2(d), where the two FSs are quite different away from the crossing points. However in this case one realizes that if at some $\mathbf{k}$ point the two bands are far apart, the effect of the SDW is very small, and we can approximate those FS parts as participating in SC pairing only, with little or no competition from the SDW interaction. This can be seen from Eq. (2.19) for the Green's function. For example, for electrons near the FS of the c band, $\xi_c\to 0$, ξ_f is large and $\hat{G}^{-1}_{cc}\approx\hat{G}^{-1}_{c0}+\mathcal{O}(m^2/\xi_f)$, and the corrections due to m can be neglected when we go along c FS away from the region where $\xi_c\approx\xi_f\approx 0$. We will return to this issue in Sec. VI, to show that the results are qualitatively the same whether we consider large or small splitting of the FSs.

For small splitting between hole and electron Fermi surfaces, we perform ξ integration analytically. For this we approximate $V^{SC}_{\mathbf{k},\mathbf{p}}$ by an isotropic V^{SC}, i.e., take angle-independent SC gap. The sign of V^{SC} can be arbitrary and we consider separately the two cases:

(a) $V^{SC}>0$: results in the s^{+-} state, with gaps of opposite signs for electrons and holes,

$$\Delta_f=-\Delta_c=\Delta \quad \text{or} \quad \Delta_+=0, \quad \Delta_-=\Delta$$

(b) $V^{SC}<0$: s^{++} state, with the same gaps on two FSs,

$$\Delta_f=\Delta_c=\Delta \quad \text{or} \quad \Delta_+=\Delta, \quad \Delta_-=0.$$

In both cases $\Delta_+\Delta_-=0$ and the denominator of the Green's function can be written as

$$D=(\varepsilon_n^2+E_+^2)(\varepsilon_n^2+E_-^2)=(\xi^2_{\mathbf{kq}}+\Sigma_+^2)(\xi^2_{\mathbf{kq}}+\Sigma_-^2), \quad (2.39)$$

where

$$\Sigma^2_\pm=\varepsilon_n^2+\Delta^2+m^2-\delta^2_{\hat{\mathbf{kq}}}\pm 2\sqrt{m^2\Delta^2\frac{1+s}{2}-\delta^2_{\hat{\mathbf{kq}}}(\varepsilon_n^2+\Delta^2)} \quad (2.40)$$

with $s=+1$ ($s=-1$) corresponding to s^{++} (s^{+-}) state. Closing the integration contours over $\xi_{\mathbf{kq}}$ in the self-consistency equations and in the free energy over the upper half-plane and counting poles at $+i\Sigma_\pm$ we obtain

$$\frac{-s}{v^{SC}}\Delta=\pi T\sum_{|\varepsilon_n|<\Lambda}\left\langle\frac{\Delta}{\Sigma_++\Sigma_-}\left(1+\frac{\varepsilon_n^2+\Delta^2+\delta^2_{\hat{\mathbf{kq}}}-sm^2}{\Sigma_+\Sigma_-}\right)\right\rangle, \quad \frac{1}{|v^{SC}|}=\ln\frac{1.13\Lambda}{T_c}, \quad (2.41)$$

$$\frac{1}{v^{SDW}}m = \pi T \sum_{|\varepsilon_n|<\Lambda} \left\langle \frac{m}{\Sigma_+ + \Sigma_-}\left(1 + \frac{\varepsilon_n^2 + m^2 - \delta_{\hat{\mathbf{kq}}}^2 - s\Delta^2}{\Sigma_+\Sigma_-}\right)\right\rangle, \quad \frac{1}{v^{SDW}} = \ln\frac{1.13\Lambda}{T_s}, \tag{2.42}$$

$$\frac{\Delta F(\Delta,m)}{4N_F} = \frac{\Delta^2}{2}\ln\frac{T}{T_c} + \frac{m^2}{2}\ln\frac{T}{T_s} - 2\pi T\sum_{\varepsilon_n>0}\left\langle \frac{1}{2}(\Sigma_+ + \Sigma_-) - \varepsilon_n - \frac{\Delta^2}{2\varepsilon_n} - \frac{m^2}{2\varepsilon_n}\right\rangle, \tag{2.43}$$

where angle brackets denote remaining momentum averaging over directions on the FS. N_F is the density of states at the FS per spin, and $v^{SC}=2N_FV^{SC}$ and $v^{SDW}=N_FV^{SDW}$ are the dimensionless couplings in the SC and SDW channels.[13] Taken alone, v^{SC} leads to a SC state with critical temperature T_c, which is independent of $\delta_{\hat{\mathbf{kq}}}$ as one can check by setting $m=0$ in Eq. (2.41), while v^{SDW} leads to an SDW state with transition temperature T_s which does depend on $\delta_{\hat{\mathbf{kq}}}$. We define T_s as the SDW transition temperature at *perfect* nesting, when $\delta_{\hat{\mathbf{kq}}}\equiv 0$.

The relative sign between SC and SDW orders, as given by terms $-s\Delta m^2$ in Eq. (2.41) and $-sm\Delta^2$ in Eq. (2.42), is positive for s^{+-} state resulting in effective attraction of the two orders and negative for s^{++} state implying that the formation of one order resists the appearance of the other.[29,41] The actual coexistence of the two orders, however, is a more subtle effect and needs to be determined from the exact solution of these equations and the analysis of the free energy. The difference in excitation energies Eq. (2.26) and Eq. (2.40) between s^{++} and s^{+-} states is also consistent with previous studies of d- and p-wave superconductivity in heavy-fermion metals[39] that concluded the SC states with symmetries $PT_Q=-1$ (e.g., s^{+-}, d), where P is parity $[P\Delta(\mathbf{p})=\Delta(-\mathbf{p})]$ and T_Q is the shift by the nesting vector $[T_Q\Delta(\mathbf{p})=\Delta(\mathbf{p}+\mathbf{Q})]$, are more likely to form coexistence with SDW than those with $PT_Q=+1$ (e.g., s^{++}, p).

We will also analyze the quasiparticle DOS, which is given by the integrals over $\xi_{\mathbf{kq}}$ of the diagonal components of the Green's function. For example, for c fermions

$$g_c(\varepsilon_n,\hat{\mathbf{k}}) = \int \frac{d\xi_{\mathbf{kq}}}{\pi} G_{cc}^{(1)} = \frac{-i\varepsilon_n}{\Sigma_+ + \Sigma_-}\left(1 + \frac{\varepsilon_n^2 + m^2 + \Delta^2 + \delta_{\hat{\mathbf{kq}}}^2}{\Sigma_+\Sigma_-}\right), \tag{2.44}$$

which for pure SDW state reduces to

$$g_c(\varepsilon_n,\hat{\mathbf{k}}) = -\frac{1}{2}\sum_{\pm}\frac{i\varepsilon_n \pm \delta_{\hat{\mathbf{kq}}}}{\sqrt{m^2 - (i\varepsilon_n \pm \delta_{\hat{\mathbf{kq}}})^2}} \tag{2.45}$$

and actual DOS is obtained by analytic continuation,

$$\frac{N(\epsilon,\hat{\mathbf{k}})}{N_F} = -\Im\mathrm{m}\, g(i\varepsilon_n \to \epsilon + i0^+,\hat{\mathbf{k}}). \tag{2.46}$$

III. PURE SDW STATE

In pnictides, parent materials usually have only magnetic order below a transition temperature T_s. Superconductivity appears at a finite doping, when the SDW transition is suppressed. Keeping this in mind, we consider first a purely SDW state, and analyze how it is modified when FSs are deformed by addition or removal of electronic carriers, and whether modified FSs are still present in the SDW phase. To remind, we denote by T_s the SDW-N transition temperature at perfect nesting, which effectively gives the scale of SDW interaction in the system. The true instability temperature, which we denote explicitly by $T_s(\delta_{\hat{\mathbf{kq}}})$, is a function of ellipticity, doping, and incommensurability.

We begin by presenting explicit formulas for the excitation spectrum, the SDW order parameter, and the free energy. For $\Delta=0$, $\Sigma_\pm^2$ given by Eq. (2.40) is

$$\Sigma_\pm^2 = (\varepsilon_n \pm i\delta_{\hat{\mathbf{kq}}})^2 + m^2 \tag{3.1}$$

and the excitation spectrum consists of four branches with energies $\pm E_\pm(\Delta=0)$, where

$$E_\pm(\Delta=0) = \sqrt{\xi_{\mathbf{kq}}^2 + m^2} \pm \delta_{\hat{\mathbf{kq}}}. \tag{3.2}$$

In Eqs. (3.1) and (3.2),

$$\xi_{\mathbf{kq}} = \frac{\xi_f(\mathbf{k}+\mathbf{q}) - \xi_c(\mathbf{k})}{2},$$

$$\delta_{\hat{\mathbf{kq}}} = \frac{\xi_f(\mathbf{k}+\mathbf{q}) + \xi_c(\mathbf{k})}{2} \approx \frac{\xi_f(\mathbf{k}_F^c+\mathbf{q})}{2} = \frac{v_F}{2}\hat{\mathbf{k}}(\mathbf{k}_F^c - \mathbf{k}_F^f + \mathbf{q}). \tag{3.3}$$

We remind that $\delta_{\hat{\mathbf{kq}}}$ describes the mismatch between the shapes of the electron and hole bands and determines their nesting properties in $\hat{\mathbf{k}}$ direction.

Equation (2.42) for the SDW order parameter m simplifies to

$$\frac{1}{v^{SDW}} = 2\pi T \sum_{0<\varepsilon_n<\Lambda} \mathrm{Re}\frac{1}{\sqrt{(\varepsilon_n + i\delta_{\hat{\mathbf{kq}}})^2 + m^2}} \tag{3.4}$$

and the cutoff Λ can be eliminated in favor of T_s,

$$\ln\frac{T}{T_s} = 2\pi T \sum_{\varepsilon_n>0} \mathrm{Re}\left\langle \frac{1}{\sqrt{(\varepsilon_n + i\delta_{\hat{\mathbf{kq}}})^2 + m^2}} - \frac{1}{|\varepsilon_n|} \right\rangle, \tag{3.5}$$

where the summation over ε_n now extends to infinity. Second-order transition temperature $T=T_s(\delta_{\hat{\mathbf{kq}}})$ is obtained by setting $m=0$,

$$\ln\frac{T}{T_s} = 2\pi T \sum_{\varepsilon_n>0} \mathrm{Re}\left\langle \frac{1}{\varepsilon_n + i\delta_{\hat{\mathbf{kq}}}} - \frac{1}{\varepsilon_n} \right\rangle. \tag{3.6}$$

The free energy, Eq. (2.43), becomes

$$\begin{aligned}\frac{\Delta F(m)}{4N_F} &= \frac{m^2}{2}\ln\frac{T}{T_s} \\ &\quad - 2\pi T \sum_{\varepsilon_n>0} \left(\mathrm{Re}\langle\sqrt{(\varepsilon_n + i\delta_{\hat{\mathbf{kq}}})^2 + m^2}\rangle - \varepsilon_n - \frac{m^2}{2\varepsilon_n} \right) \\ &= \frac{m^2}{2}\ln\frac{1.13\Lambda}{T_s} \\ &\quad - 2\pi T \sum_{0<\varepsilon_n<\Lambda} (\mathrm{Re}\langle\sqrt{(\varepsilon_n + i\delta_{\hat{\mathbf{kq}}})^2 + m^2}\rangle - \varepsilon_n).\end{aligned} \tag{3.7}$$

Below we consider several special cases for $\delta_{\hat{\mathbf{kq}}}$ (see Fig. 2).

(1) Two coaxial circles, $\mathbf{q}=0$: $\mathbf{k}_F^c - \mathbf{k}_F^f = \hat{\mathbf{k}}(k_F^c - k_F^f)$,

$$\delta_{\hat{\mathbf{kq}}} = \frac{1}{2} v_F |k_F^c - k_F^f| \equiv \delta_0. \tag{3.8}$$

For a fixed δ_0, circular hole and electron FSs survive in the SDW phase when $m<\delta_0$ [Fig. 2(b)] but come closer to each other as m increases and merge at $m=\delta_0$. At larger m all excitations are gapped [Fig. 2(a)].

(2) FS of different shapes, e.g., one circle and one ellipse, cocentered: $\mathbf{q}=0$ with $\mathbf{k}_F^c - \mathbf{k}_F^f = \hat{\mathbf{k}}(k_F^c - k_F^f + \Delta k \cos 2\phi)$,

$$\delta_{\hat{\mathbf{kq}}} = \delta_0 + \delta_2 \cos 2\phi, \quad \delta_2 = \frac{1}{2} v_F \Delta k. \tag{3.9}$$

In this case, at small enough m, the FS has a form of two hole and two electron pockets. As m gets larger, the pockets shrink and eventually disappear.

(3) Two circles of different radii, centers shifted by $\mathbf{q}$,

$$\delta_{\hat{\mathbf{kq}}} = \delta_{\hat{\mathbf{k}}} = \delta_0 + \frac{1}{2}\mathbf{v}_F\mathbf{q} = \delta_0 + \frac{1}{2} v_F q \cos(\phi - \phi_0), \tag{3.10}$$

where ϕ and ϕ_0 are the directions of $\mathbf{v}_F$ and $\hat{\mathbf{q}}$. In this case, when m increases, gapless excitations survive along a pocket in one region of the $\mathbf{k}$ while excitations with $-\mathbf{k}$ become gapped [Fig. 2(c)]. At large enough m, modified FS disappears and excitations with all momenta $\mathbf{k}$ become gapped. This scenario refers to the case when the magnetic ordering occurs at a vector, different from the nesting vector $\mathbf{Q}_0$, producing incommensurate SDW state. It may occur because the electronic system has an option to choose $\mathbf{q}\neq 0$ if it minimizes the energy or because the SDW interaction is peaked at a fixed $\mathbf{Q}\neq\mathbf{Q}_0$ for some reason. Note that Eq. (3.5) for SDW order is a magnetic analog of Fulde-Ferrell-Larkin-Ovchinnikov (FFLO) state[56] in a paramagnetically limited superconductor. An incommensurate SDW state at finite dopings has been studied in application to chromium and its alloys[57–59] and, more recently, to pnictide materials.[42,60]

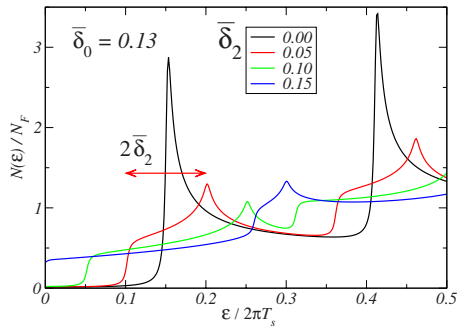

FIG. 3. (Color online) The FS averaged DOS for pure SDW state and FS mismatch $\delta_{\hat{\mathbf{kq}}}=\delta_0+\delta_2\cos 2\phi$. We use dimensionless variables denoted by bars, $\bar\delta_0=\delta_0/2\pi T_s=0.13$, zero-temperature SDW gap $\bar m_0=m(T=0)/2\pi T_s=0.28$ and vary $\bar\delta_2=\delta_2/2\pi T_s$. For $\bar\delta_2=0$, $N(\epsilon)$ vanishes below $\bar\epsilon=\bar m-\bar\delta_0$ and has two sharp BCS peaks at $\bar\epsilon=\bar m\pm\bar\delta_0$. At finite $\bar\delta_2$, each of the two peaks splits into a "band" bounded by two weaker nonanalyticities separated by $2\bar\delta_2$. The gap in the DOS behaves as $\bar m-\bar\delta_0-\bar\delta_2$ and closes when $\bar\delta_0+\bar\delta_2\geq\bar m$, metallic states forms. The DOS remains the same if we replace the ellipticity parameter $\bar\delta_2$ by the incommensurability parameter $\bar q$.

In general, all three terms are present and

$$\delta_{\hat{\mathbf{kq}}} = \delta_0 + \delta_2 \cos 2\phi + \frac{1}{2} v_F q \cos(\phi - \phi_0). \tag{3.11}$$

In the figures we use dimensionless parameters that are denoted by a bar. For isotropic and anisotropic FS distortions,

$$\bar\delta_{0,2} = \frac{\delta_{0,2}}{2\pi T_s}, \quad \bar q = \frac{v_F q}{4\pi T_s} \tag{3.12}$$

and similarly for other energy variables,

$$\bar m = \frac{m}{2\pi T_s}, \quad \bar\epsilon = \frac{\epsilon}{2\pi T_s}, \quad \bar\Delta = \frac{\Delta}{2\pi T_c}. \tag{3.13}$$

We use different notations for prefactors of $\cos(\phi-\phi_0)$ and $\cos 2\phi$ terms to emphasize that they have different origin: δ_2 is an "input" parameter defined by the elliptic form of the electron FS due to the electronic band structure while q is adjustable parameter that minimizes the free energy of the system. If the minimum of the free energy corresponds to $q=0$, SDW order is commensurate, otherwise SDW order is incommensurate.

In Fig. 3 we show the DOS $N(\epsilon)$ for the fixed $\bar\delta_0=0.13$ and $\bar m=0.28$, and different δ_2. For $\delta_2=0$, $N(\epsilon)$ vanishes below $\epsilon=m-\delta_0$ and has two BCS-type peaks at $\epsilon=m\pm\delta_0$. At finite δ_2, each of the two peaks spreads into a region of width $2\delta_2$ bounded by two weaker nonanalyticities. The gap in the DOS behaves as $m-\delta_0-\delta_2$ and closes when $\delta_0+\delta_2$ become larger than m. The DOS and all other results remain the same

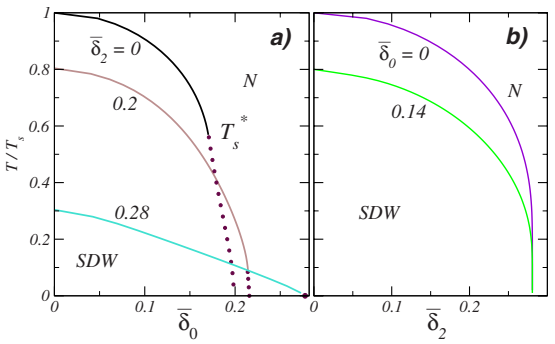

FIG. 4. (Color online) The SDW-N transition for commensurate SDW order. The parameters $\bar{\delta}_0$ and $\bar{\delta}_2$ describe the difference between the area of hole and electron pockets and the ellipticity of the electron pocket, respectively. Here and in all subsequent figures dotted lines mark first-order transitions, solid and dashed lines mark second-order transitions. Panel (a): variation in the transition temperature with δ_0 for fixed δ_2. The transition is second order at small δ_0 but becomes first order at larger δ_0. At $\delta_2=0$, the transition becomes first order at $T_s^* \approx 0.56 T_s$. Panel (b): variation in the transition temperature with δ_2 for fixed δ_0. $T_s(\delta_0, \delta_2)$ monotonically decreases with increasing δ_2 and vanishes at the same value $\bar{\delta}_2 \approx 0.28073$, independent of δ_0.

if we replace the ellipticity parameter $\bar{\delta}_2$ by the incommensurability parameter $\bar{q}$ because the angular integral in Eq. (2.45) or Eq. (3.6) over momentum directions on the FS coincides for $\cos(\phi-\phi_0)$ and $\cos 2\phi$ terms in $\hat{\delta_{\mathbf{k},\mathbf{q}}}$, if considered separately. The DOS and $T_s(\hat{\delta_{\mathbf{kq}}})$ change, however, when both δ_2 and q are present simultaneously.

Below we discuss the phase diagram for the pure SDW state to the extend that we will need to analyze potential coexistence between SDW and SC states, which is the subject of this paper.

It is instructive to consider separately the case when SDW order is set to remain commensurate for all $\delta_{0,2}$ (i.e., $q=0$) and the case when the system can choose q. In our model, the first case is artificial and just sets the stage to study the actual situation when the value of q is obtained by minimizing the free energy. However, a commensurate magnetic order may be stabilized in the SDW state, if the interaction V^{SDW} is by itself sharply peaked at the commensurate momentum $\mathbf{Q}_0$.

The results for the case $q \equiv 0$ are presented in Fig. 4. In panel (a) we present the results for the transition temperature $T_s(\delta_0, \delta_2)$ for several values of δ_2. All curves show that the transition is second order at high T and first order at small T. The first-order transition lines [dotted lines in Fig. 4(a)] were obtained by solving numerically the nonlinear equation for m, substituting the result into the free energy [Eq. (3.7)] and finding a location where $\Delta F(m)=0$.

To verify that the transition becomes first order at low T, we expanded the free energy in powers of m as

$$\Delta F(m) = \alpha_m m^2 + B m^4 + \cdots \tag{3.14}$$

and checked the sign of the B term. The coefficients α_m and B are determined from Eq. (3.7),

$$\alpha_m = \frac{1}{2}\left(\ln\frac{T}{T_s} - 2\pi T \sum_{\varepsilon_n>0} \mathrm{Re}\left\langle \frac{1}{\varepsilon_n + i\hat{\delta_{\mathbf{k}}}} - \frac{1}{\varepsilon_n} \right\rangle \right),$$

$$B = \frac{\pi T}{4} \sum_{\varepsilon_n>0} \mathrm{Re}\left\langle \frac{1}{(\varepsilon_n + i\hat{\delta_{\mathbf{k}}})^3} \right\rangle, \tag{3.15}$$

where $\hat{\delta_{\mathbf{k}}} = \delta_0 + \delta_2 \cos 2\phi$. Solid lines in Fig. 4(a) correspond to $\alpha_m=0$. The N-SDW transition is second order and occurs when $\alpha_m=0$ if $B>0$ but becomes first order and occurs before α_m becomes negative if $B<0$. We indeed found that for *all* fixed δ_2, for which SDW-N transition is possible, B changes sign along the line $\alpha_m=0$ and becomes negative at small T. For $\delta_2=0$, this occurs at $T_s^*=0.56T_s$ and $\bar{\delta}_0^*=0.17$.

We point out the following counterintuitive feature in Fig. 4(a). Increase in δ_2 reduces the transition temperature at $\delta_0=0$ and at the same time makes the curve flatter allowing for a larger SDW region along δ_0. The transition line becomes completely flat at a critical value $\delta_{2c}=0.28073(2\pi T_s)$ (see below) when $T_s(\delta_0, \delta_{2c})=+0$. At this point, it spans the interval $\delta_0 \in [0, \delta_{2c}]$. The existence of the SDW ordered state at $\delta_2=\delta_{2c}$ over a finite range of δ_0 despite that the transition temperature is +0 is a highly nontrivial effect which deserves a separate discussion.[61]

In Fig. 4(b) we show the transition temperature at fixed δ_0, as a function of the ellipticity parameter δ_2. As expected, $T_s(\delta_2)$ monotonically decreases with increasing ellipticity of the electron band. The SDW order exists up to δ_{2c}, at which $T_s(\delta_{2c})=+0$. The value of δ_{2c} is independent of δ_0 and can be obtained by taking the limit $T \to 0$ in Eq. (3.4) with $m=0$ and rewriting this equation as

$$\frac{1}{v^{SDW}} = \mathrm{Re}\int_0^\Lambda d\varepsilon \left\langle \frac{1}{\varepsilon + i\hat{\delta_{\mathbf{k}}}} \right\rangle = \mathrm{Re}\ln\frac{2\Lambda}{i\delta_0 + \sqrt{\delta_2^2 - \delta_0^2}}. \tag{3.16}$$

The interaction can be eliminated in favor of zero-temperature gap m_0 at $\delta_0=\delta_2=0$

$$\frac{1}{v^{SDW}} = \int_0^\Lambda d\varepsilon \frac{1}{\sqrt{\varepsilon^2 + m_0^2}} = \ln\frac{2\Lambda}{m_0}, \tag{3.17}$$

where from Eq. (3.5) we obtain,

$$m_0 = \frac{2\pi T_s}{2e^{\gamma_E}} = 0.28073 \times (2\pi T_s) \tag{3.18}$$

and $\gamma_E \approx 0.57722$ is Euler's constant. At finite δ_0 and δ_2, the value of m at $T=0$ remains equal to m_0 as long as $\delta_0+\delta_2 < m_0$, and becomes smaller than m_0 outside this range. The combination of Eqs. (3.16) and (3.17) gives $\delta_{2c}=m_0 = 0.28073 \times (2\pi T_s)$, provided that $\delta_0 < \delta_{2c}$. Another solution $\delta_2^2 = 2\delta_0 m_0 - m_0^2$ at $m_0/2 < \delta_0 < m_0$ corresponds to an unstable state. A similar result has been obtained in the studies of FFLO transition.[56,62]

The form of $T_s(\delta_2)$ near δ_{2c} can be obtained analytically by rewriting the condition $\alpha_m=0$ in (3.15) as

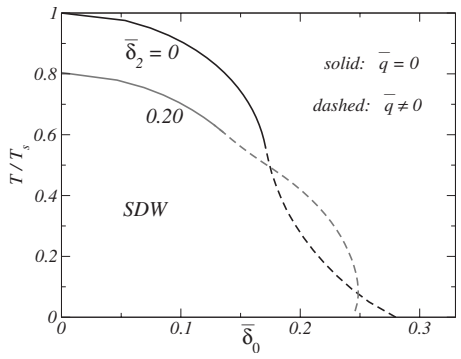

FIG. 5. Same as in Fig. 4 but when the system is allowed to choose between commensurate and incommensurate SDW orders. Solid lines are second-order transition lines into a state with a commensurate SDW order and dashed lines are second-order transition lines into an SDW state with an incommensurate SDW order (the magnetic analog of FFLO state). For all $\delta_2>0$, incommensuration occurs before the commensurate transition becomes first order (the onsets of incommensuration and first-order transition coincide for $\delta_2=0$). Observe that incommensuration develops at progressively smaller δ_0 as δ_2 increases and $T_s(\delta_0)$ decreases but the range of δ_0 over which incommensurate SDW order exists actually increases with increasing δ_2.

$$\ln\frac{T}{T_s}+2\pi T\sum_{\varepsilon_n>0}\left\langle\frac{\delta_2^2\cos^2 2\phi}{\varepsilon_n(\varepsilon_n^2+\delta_2^2\cos^2 2\phi)}\right\rangle=0, \quad (3.19)$$

integrating explicitly over ϕ, re-expressing $1/\sqrt{\varepsilon_n^2+\delta_2^2}$ as $(2/\pi)\int_0^\infty dx/(x^2+\varepsilon_n^2+\delta_2^2)$, and performing the summation over ε_n before the integration over x. Carrying out this procedure, we obtain

$$T_s(\delta_2)\approx\frac{\delta_{2c}}{|\ln(1-\delta_2/\delta_{2c})|}. \quad (3.20)$$

We see that T_s very rapidly increases at deviations from δ_{2c}. For $\delta_2=0.9974\delta_{2c}$ ($\bar{\delta}_2=0.28$), Eq. (3.20) yields $T_s(\delta_2)\approx 0.3T_s$, in good agreement with Fig. 4(a).

Also, one can easily show that at $T=0$ fermionic excitations in the SDW state are all gapped when $m_0>\delta_0+\delta_2$. When $\delta_0+\delta_2>m_0$, the SDW state possess Fermi surfaces and gapless fermionic excitations.

We next consider the case when the system is free to choose between commensurate and incommensurate SDW orders and may develop incommensurate order to lower the free energy. In Fig. 5 we show the transition temperature $T_s(\delta_0)$ for fixed δ_2. We found that, for all δ_2, first-order transition is overshadowed by a transition into an incommensurate SDW state. For $\delta_2=0$, incommensuration develops exactly where B changes sign and the transition into incommensurate SDW state remains second order for all δ_0. For $\delta_2>0$, incommensuration develops before B changes sign, and the transition into incommensurate SDW state remains second order over some range of δ_0 but eventually becomes first order at large δ_0 and low T. The full phase diagram also contains a transition line (not shown in Fig. 5) separating already developed commensurate and incommensurate SDW orders.

To analyze the interplay between the appearance of incommensurate SDW order and the sign change in B, we again expand the free energy in powers of m but now allow incommensuration parameter δ_1 to be nonzero, i.e., replace in the coefficients in Eq. (3.14), $\delta_{\hat{\mathbf{k}}}=\delta_0+\delta_2\cos(2\phi)$ with $\delta_{\hat{\mathbf{k}},\mathbf{q}}=\delta_{\hat{\mathbf{k}}}+q\cos(\phi-\phi_0)$. In general, for small q,

$$\alpha_m(\delta_{\hat{\mathbf{k}},\mathbf{q}})=\alpha_0(\delta_{\hat{\mathbf{k}}})+\alpha_2(\delta_{\hat{\mathbf{k}}})q^2+\alpha_4(\delta_{\hat{\mathbf{k}}})q^4+\mathcal{O}(q^6) \quad (3.21)$$

with $\alpha_0(\delta_{\hat{\mathbf{k}}})$ given by Eq. (3.15). When α_4 and B are positive, the N-SDW transition is second order, and is into a commensurate SDW state when $\alpha_2>0$ and into an incommensurate SDW state when α_2 changes sign and becomes negative. If B changes sign while α_2 is still positive, the SDW-N transition becomes first order before incommensuration develops.

To understand the phase diagram, it is sufficient to consider small δ_2. Expanding all coefficients in powers of δ_2 we obtain

$$\alpha_0(\delta_{\hat{\mathbf{k}}})=\alpha_{0,0}+\alpha_{0,2}\delta_2^2+\mathcal{O}(\delta_2^4), \quad (3.22a)$$

$$\alpha_2(\delta_{\hat{\mathbf{k}}})=\alpha_{2,0}+\alpha_{2,1}\cos 2\phi_0\delta_2+\mathcal{O}(\delta_2^2), \quad (3.22b)$$

$$\alpha_4(\delta_{\hat{\mathbf{k}}})=\alpha_{4,0}+\mathcal{O}(\delta_2^2),$$

$$B=\frac{1}{2}\alpha_{0,2}+\mathcal{O}(\delta_2^2), \quad (3.22c)$$

where

$$\alpha_{0,0}=\frac{1}{2}\left(\ln\frac{T}{T_s}+2\pi T\sum_{\varepsilon_n>0}\frac{\delta_0^2}{\varepsilon_n(\varepsilon_n^2+\delta_0^2)}\right), \quad (3.23a)$$

$$\alpha_{2,0}=\alpha_{0,2}=\frac{1}{4}2\pi T\sum_{\varepsilon_n>0}\varepsilon_n\frac{\varepsilon_n^2-3\delta_0^2}{(\varepsilon_n^2+\delta_0^2)^3}, \quad (3.23b)$$

$$\alpha_{2,1}=\frac{3}{2}2\pi T\sum_{\varepsilon_n>0}\frac{\varepsilon_n(\delta_0^2-\varepsilon_n^2)\delta_0}{(\varepsilon_n^2+\delta_0^2)^4}, \quad (3.23c)$$

$$\alpha_4=-\frac{3}{16}2\pi T\sum_{\varepsilon_n>0}\varepsilon_n\frac{\varepsilon_n^4-10\delta_0^2\varepsilon_n^2+5\delta_0^4}{(\varepsilon_n^2+\delta_0^2)^5}. \quad (3.23d)$$

We see from Eq. (3.22) that for $\delta_2=0$, B and $\alpha_2(\delta_{\hat{\mathbf{k}}})$ change sign simultaneously, at the point where $\alpha_{2,0}=\alpha_{0,2}=0$. However, when $\delta_2\neq 0$, $\alpha_2(\delta_{\hat{\mathbf{k}}})$ changes sign before B becomes negative because $\alpha_2(\delta_{\hat{\mathbf{k}}})$ contains a term linear in δ_2, whose prefactor can be made negative by adjusting ϕ_0. This explains why in Fig. 5 incommensuration begins while B is still positive. Also, we verified that near the onset points for incommensuration, $\alpha_4(\delta_{\hat{\mathbf{k}}})>0$, i.e., in this range the transition into incommensurate SDW is second order. At larger δ_0, the incommensurate transition eventually becomes first order.

IV. SDW+SC STATE, NUMERICAL ANALYSIS

In the next two sections we look at potential coexistence of SDW and the s^{+-} or s^{++} states, when the system is doped

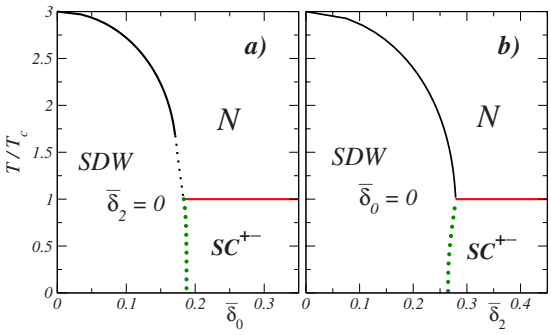

FIG. 6. (Color online) The phase diagram of SDW and SC s^{+-} states when only a commensurate SDW order is allowed ($q=0$). We set $T_s/T_c=3$ and varied either (a) the relative radius of circular hole and electron pockets or (b) the form of one of the pockets. The pure SC s^{+-} and SDW states are separated by first-order transition, and there is no co-existence region (Refs. 41 and 42).

and the SDW order is suppressed. The superconducting T_c is doping independent, so at some doping SDW and SC transition temperatures cross. Near this point, the two orders either support or suppress each other and either coexist or are separated by a first-order transition.

In this section we present numerical results in the extended range of temperatures and dopings and in the next section we corroborate them with analytical consideration in the vicinity of the crossing point, when both order parameters are small, and at $T=0$.

A. Coexistence with $s^{\pm}$ state

We look first at the s^{+-} state. In this case the system of coupled self-consistency equations for Δ and m is obtained from Eqs. (2.41)–(2.43) by taking $\Sigma_{\pm}^2=(E_n \pm i\hat{\delta_{\mathbf{kq}}})^2+m^2$ and $E_n=\sqrt{\varepsilon_n^2+\Delta^2}$,

$$\ln\frac{T}{T_c}=2\pi T\sum_{\varepsilon_n>0}\mathrm{Re}\left\langle\frac{(E_n+i\hat{\delta_{\mathbf{kq}}})/E_n}{\sqrt{(E_n+i\hat{\delta_{\mathbf{kq}}})^2+m^2}}-\frac{1}{|\varepsilon_n|}\right\rangle, \tag{4.1a}$$

$$\ln\frac{T}{T_s}=2\pi T\sum_{\varepsilon_n>0}\mathrm{Re}\left\langle\frac{1}{\sqrt{(E_n+i\hat{\delta_{\mathbf{kq}}})^2+m^2}}-\frac{1}{|\varepsilon_n|}\right\rangle. \tag{4.1b}$$

We remind that T_c is the transition temperature for the pure SC state and T_s is the transition temperature for the pure SDW state at $\hat{\delta_{\mathbf{kq}}}=0$.

These equations are solved numerically to find all possible states (Δ,m) and their energies evaluated using Eq. (2.43). The main results for this part are presented in Figs. 6–12.

1. Commensurate SDW state

Figure 6 shows the results for the case when SDW order is set to be commensurate (i.e., $q=0$) and the FSs are either coaxial circles [panel (a)] or of different shapes with equal k_F (panel b). In the first case, $\delta_2=0$ and $\delta_0\neq 0$, and in the second case $\delta_0=0$ and $\delta_2\neq 0$. We see that in both cases pure SDW and SC states are separated by a first-order transition. We verified that in both cases fermionic excitations in the SDW state are fully gapped at $T=0$ and thus there are no Fermi surfaces. From this perspective, the results presented in Fig. 6 are consistent with the idea that coexistence requires the presence of the Fermi surfaces in the SDW state. However, we will see next that the situation in the cases when both δ_0 and δ_2 are nonzero is more complex.

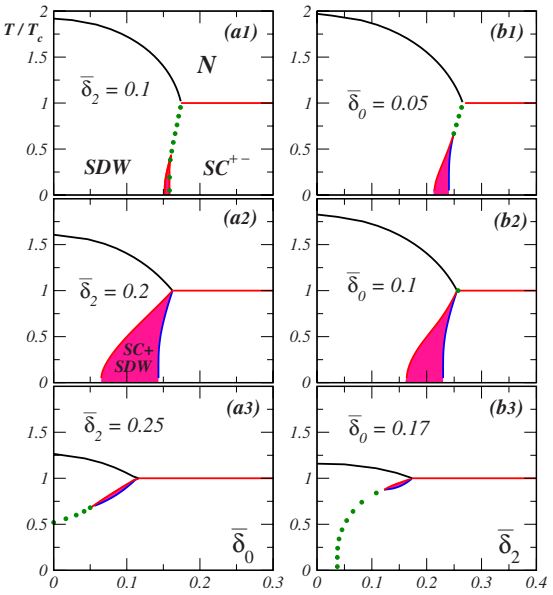

FIG. 7. (Color online) Appearance of coexistence when both δ_0 and δ_2 are finite. We set $T_s/T_c=2$ and $q=0$. Panels (a1)–(a3)—phase diagrams in variables T,δ_0 at fixed δ_2 and panels (b1)–(b3)—phase diagrams in variables T,δ_2 at fixed δ_0. Panels (a1) and (b1)—there appears a region near $T=0$, where SDW and SC s^{+-} orders coexist. Panels (a2) and (b2)—the coexistence region broadens and reaches $T=T_c$. Panels (a3) and (b3)—the transition at low T becomes first order between pure SDW and SC states but narrow coexistence region is still present near T_c. A complimented zero-temperature phase diagram is presented in Fig. 10.

This is demonstrated in Fig. 7 which shows the phase diagram for $T_s/T_c=2$ as a function of δ_0 for a set of fixed δ_2 [panels (a1)–(a3)] and as a function of δ_2 for a set of fixed δ_0 [panels (b1)–(b3)]. For all cases, pure SDW state is fully gapped at $T=0$, so naively one should not expect a coexistence state. However, as is evident from the figure, the phase diagram does involve the coexistence phase, which can be either at low T (including $T=0$), or near $T=T_c$, depending on the parameters. In particular, as δ_2 in panels (a) or δ_0 in panels (b) increase, the coexistence state first appears at low T while at higher T the pure SDW and SC states are still separated by first-order transition [panels (a1) and (b1)]. Then the coexistence region grows and extends up to $T=T_c$ [panels (a2) and (b2)]. At even larger δ_2 or δ_0, SDW and SC states are separated by the first-order transition at low T but the coexistence phase still survives near T_c.

In Fig. 8 we show the phase diagram for $\bar{\delta}_2=0.2$ and $T_s/T_c=5$ together with the plots of SDW and SC order parameters and the free energy. We see the same behavior as in Fig. 7(a2)—there is a coexistence phase for all T up to T_c. In

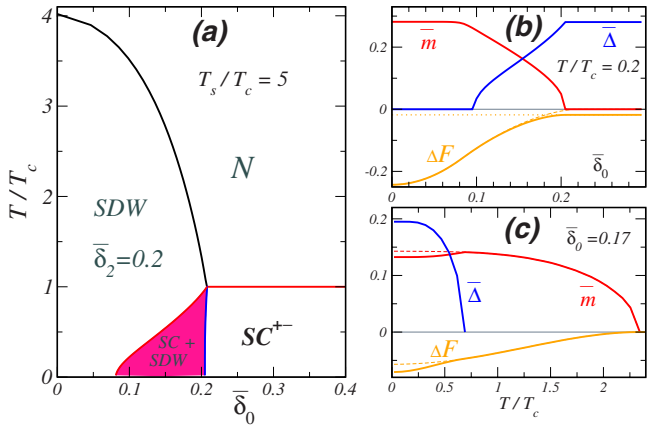

FIG. 8. (Color online) (a) Same as in Fig. 7(b) but for $T_s/T_c=5$. [(b) and (c)] SDW and SC gaps, in units $\bar{m}$ and $\bar{\Delta}=\Delta/2\pi T_c$, and the free energy (b) as functions of $\bar{\delta}_0$ along the line $T/T_c=0.2$, and (c) as functions of temperature for $\bar{\delta}_0=0.17$.

Fig. 9 we show the changes in the quasiparticle DOS at low $T=0.1T_c$ as the system evolves from the SDW state to the SC state via the coexistence region.

Finally, in Fig. 10, we show the zero-temperature phase diagram in variables δ_0 and δ_2 for $T_s/T_c=2$ and $T_s/T_c=5$, together with the locus of points, where $T_s(\delta_0,\delta_2)=T_c$. The phase diagram was obtained by numerically solving Eq. (4.1) and evaluating the free energy at $T/T_c=0.02$. This phase diagram corroborates the results of Figs. 7 and 8—the zero T behavior in panels (a) and (b) in Fig. 7 is obtained by taking either horizontal or vertical cuts in Fig. 10. In particular, we

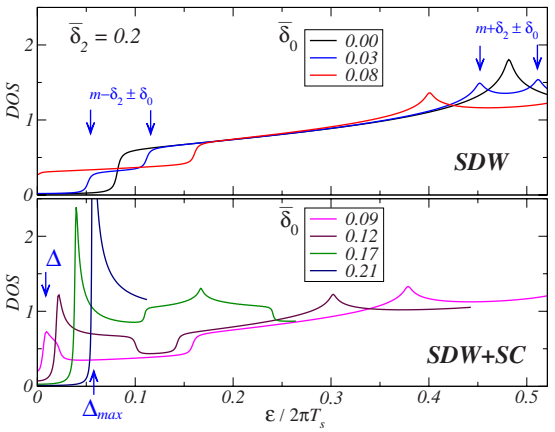

FIG. 9. (Color online) FS averaged DOS as a function of energy at $T/T_c=0.1$ for different values of δ_0 (i.e., different dopings). We set $\bar{\delta}_2=0.2$ and $T_s/T_c=5$. The characteristic values of the SDW order parameter for this range of parameters is $\bar{m}\approx 0.28$ (zero-T limit). Upper panel: DOS for small $\bar{\delta}_0$, when the system remains in the pure SDW state. This figure is similar to Fig. 3. The DOS vanishes below $\epsilon=m-\delta_0-\delta_2$ and has logarithmic nonanalytic behavior at $\epsilon=m\pm\delta_0+\delta_2$, and sudden drops at $\epsilon=m\pm\delta_0-\delta_2$. Lower panel: DOS for larger δ_0, when SDW and SC orders coexist. Sharp peaks at small ϵ are due to opening of the superconducting gap Δ. Once SDW order disappears at $\bar{\delta}_0\approx 0.21$, the DOS acquires BCS form with the maximal gap $\Delta_{max}/2\pi T_c\approx 0.28$.

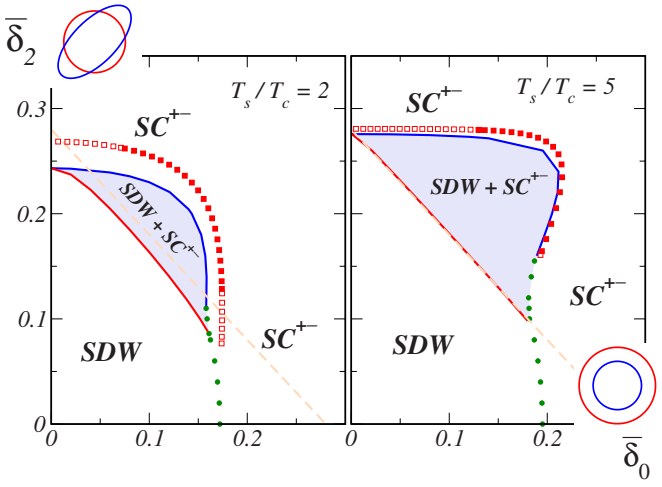

FIG. 10. (Color online) The zero-temperature phase diagram: SDW, SC states and their coexistence region for various δ_2 and δ_0 and two different $T_s/T_c=2$ (left) and $T_s/T_c=5$ (right). We only allow the system to develop a commensurate SDW order ($q=0$). The dashed line denotes first appearance of gapless excitations in the pure SDW state [$m=\delta_0+\delta_2$, Eq. (2.45)]. The coexistence region at $T=0$ (shaded area) extends down to $\delta_0=0$ but is not present at small δ_2. The width of the coexistence region increases with the relative strength of SDW interaction, as determined by ratio T_s/T_c. The squares mark the location of the crossing point between $T_s(\delta_0,\delta_2)$ and T_c. Open squares indicate that the SDW-SC transition near T_c is first order while filled squares signal the presence of the coexistence phase near T_c. Note that the regions where coexistence phase is present at $T=0$ and near T_c are not identical.

see from Fig. 10 that the transformation between panels (a2) and (a3) of Fig. 7 is such that the coexistence region at $T=0$ first moves to the left, shrinks, and disappears at $\bar{\delta}_2\approx 0.24$. Similarly, in panels (b), the coexistence range shrinks to a point at $\bar{\delta}_0\approx 0.16$ and at larger δ_0 the transition between SDW and SC phases at $T=0$ becomes first order. In the next section we present the results of complimentary analytical studies of the phase diagram at $T=0$ and near T_c. These results are in full agreement with the numerical analysis in this section.

Observe that for $T_s/T_c=5$ the left boundary of the coexistence region is located very close to the line $\delta_0+\delta_2=m_0$ (dashed line in Fig. 10, $\bar{\delta}_0+\bar{\delta}_2=0.28073$), at which gapless excitations and Fermi surfaces appear in the SDW state. For this T_s/T_c, the coexistence region at $T=0$ virtually coincides with the region where SDW state has a Fermi surface. However, for smaller $T_s/T_c=2$ (Fig. 7; left panel in Fig. 10), coexistence clearly occurs already in the parameter range where SDW excitations are all gapped. The coexistence for $T_s/T_c=2$ is therefore not the result of the "competition for the Fermi surface" but rather the consequence of the fact that the system can gain in energy by reducing the SDW order parameter (still keeping all fermionic excitations gapped) and creating a nonzero SC order parameter. The gain of energy in this situation can best be interpreted as the consequence of the effective attraction between the two orders.

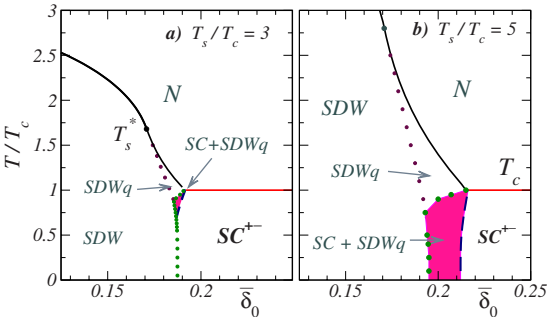

FIG. 11. (Color online) The phase diagram for $\delta_2=0$, when the system can choose the value of **q**. Incommensurate SDW order appears below $T_s^*=0.56T_s$ and leaves some parts of the FS ungapped, allowing for coexisting SC order. (a) $T_s/T_c=3$. The SDW+SC phase appears only in a small region near T_c. At low T the system still undergoes a first-order transition between commensurate SDW and SC states. (b) For larger $T_s/T_c=5$ (weaker SC interaction) the coexistence region widens and extends down to $T=0$. The $q=0$ SDW state has the lowest energy at $T=0$ for $\bar{\delta}_0 \lesssim 0.195$.

2. Commensurate vs incommensurate SDW state

One of the results of our consideration so far is that, if we keep an SDW order commensurate, a finite region of SDW+SC phase appears only when both δ_0 and δ_2 are nonzero. If we allow the system to choose the ordering momentum of the SDW state, the coexistence region widens and appears even if we set $\delta_2=0$. We illustrate this in Fig. 11, where we plot the phase diagram at $\delta_2=0$ for two different values of T_s/T_c. In agreement with Fig. 5, at $T<T_s^*$, the system chooses an SDW state with a nonzero q. We see that, in this situation, there appears a region where SC state coexist with an incommensurate SDW state.[42] The coexistence region widens up when the ratio T_s/T_c increases and for large enough T_s/T_c extends down to $T=0$. In Fig. 12 we set δ_2 to be nonzero ($\bar{\delta}_2=0.2$) and allowed the system to choose q

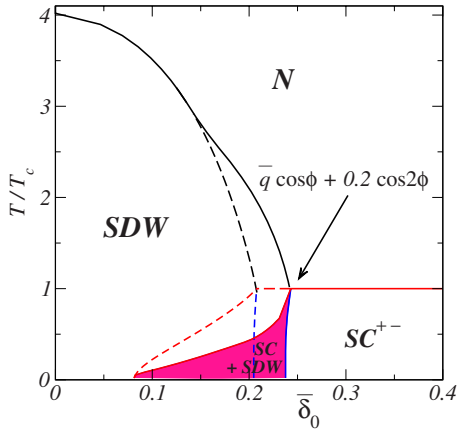

FIG. 12. (Color online) Same as in Fig. 8(a) but now we allow the system to choose the value of q. The phase diagram from Fig. 8 is shown by dashed lines. A finite q emerges below a particular T and moves the coexistence region to larger δ_0, together with the SDW-N transition. This broadens the coexistence region and slightly changes the shape of $T_c(\delta_0)$ inside the magnetic dome.

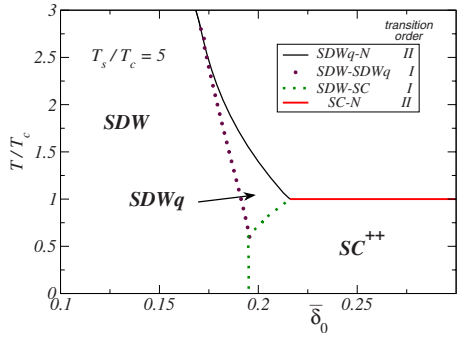

FIG. 13. (Color online) The phase diagram for a conventional s^{++} SC order parameter, at $\delta_2=0$, and varying δ_0. We allow the system to choose q. The SDW+SC state does not appear, even when SDW order becomes incommensurate.

which minimizes the free energy. The results are quite similar to the case when $q=0$. We see that the SDW and SC orders do coexists in the parameter range which extends from the crossing point down to $T=0$. The width of the coexistence region widens a bit when we allow the system to choose q, but qualitatively, the behavior in Figs. 8 and 12 is the same. Note, in our two-band model, the ellipticity of the electron FS breaks the rotational symmetry and favors the direction of **q** along the ellipse's major axis, see Eq. (3.22b).

To summarize, SDW and SC^{+-} phases do coexist in a range of finite dopings but the width of the coexistence region depends on the amount of ellipticity of the electron band and the ratio of T_s/T_c. At larger T_s/T_c the width of the coexistence region increases for fixed δ_2 and there is optimal δ_2 at which the width is the largest. The fact that the system can lower the energy by making SDW order incommensurate also acts in favor of coexistence but qualitatively the picture remains the same as in the case when q is set to be zero.

B. Minimal coexistence with s^{++} state

We next look at the SC state with gaps of the same signs on two FSs. Such states seem unlikely for pnictides because they require a negative sign of the interband pair hopping term.[13] Still, it would be interesting to investigate consequences of attractive SC interaction between electron and hole bands.

The expressions for $\Sigma_\pm$ in this case is slightly more complicated and less illuminating than those for s^{+-} state, although quite similar, and so are the self-consistency equations, which we do not write here but which are obtained from Eqs. (2.41)–(2.43) in a way completely analogous to Eqs. (4.1). We first present the results for $\delta_2=0$, Fig. 13. We found that coexistence region does not appear even if we allow SDW order to become incommensurate. There are commensurate and incommensurate SDW phases on the phase diagram, and SC^{++} phase, but the transition between SC and SDW phases remains first order. In other words, the appearance of gapless excitations in the SDW phase due to incommensuration at large δ_0 does not seem to favor a mixed superconducting and magnetic state, in sharp contrast to the case of s^{+-} SC, where incommensuration induces coexistence, see Fig. 11(b).

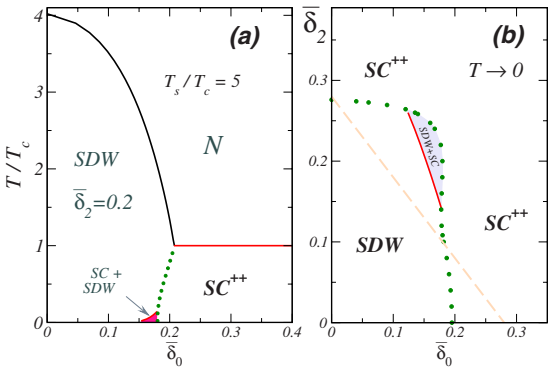

FIG. 14. (Color online) (a) Same as in Fig. 13 but for fixed $\bar{\delta}_2=0.2$ and $q=0$. For most of the phase diagram, the behavior is the same as for $\delta_2=0$ but there appears a very tiny range of SC+SDW phase at the lowest T. The transition to purely SC state is first order at all T. (b) The zero-temperature phase diagram. SDW and SC s^{++} states are separated by first-order transition virtually everywhere except a small region at finite δ_0 and δ_2, where SDW+SC state emerges.

For a nonzero δ_2, there might appear a tiny region of coexistence at low temperatures. We illustrate this in Fig. 14, where in panel (a) we plot the phase diagram for $\bar{\delta}_2=0.2$ and set $q=0$. (When the system is allowed to choose q, the results change minimally, in a way similar to Fig. 12). In panel (b) of this figure we show where the region of SDW+SC^{++} exists for different δ_0 and δ_2. We see that the range of coexistence is very narrow and we also found that the difference in free energies between a pure SDW state and SDW+SC state is very small due to small value of the SC order parameter.

Observe also that the coexistence region in Fig. 14 is to the left of the line $\delta_0+\delta_2=m_0$ at which a Fermi surface appears in the SDW state [a dashed line in Fig. 14(b)]. In other words, s^{++} superconductivity does not emerge even when there is a Fermi surface in the SDW state. This shows once again that the presence or absence of the Fermi surface in the SDW state is not the primary reason for the presence or absence of the SDW+SC phase. The true reason is energetic—the SDW+SC state can either lower or increase the energy compared to pure state depending on whether SDW and SC orders attract or repel each other. The absence of the coexistence phase even in the range where SDW state has a Fermi surface is a clear indication that there is the "repulsion" between SDW and SC orders, if the SC order is s^{++}, Eqs. (2.41) and (2.42). The same conclusion was recently reached by Fernandes *et al.*[29]

V. SDW+SC, ANALYTICAL RESULTS

We corroborate the numerical analysis in the preceding section with the analytical analysis. We first present the results of Ginzburg-Landau (GL) description near the point where second-order SDW-N and SC-N transitions meet, then consider the phase diagram at $T=0$, and finally combine the two sets of results and compare analytical phase diagram with Fig. 7.

A. Ginzburg-Landau analysis

We begin with the GL analysis near the point where $T_s(\delta_0,\delta_2)=T_c$. Near this point, both the SDW and SC order parameters are small and we can expand the free energy, Eq. (2.43), to the fourth order in m and Δ and compare different phases. For simplicity, in this section we assume that the SDW order is commensurate. An extension to a finite q complicates the formulas but does not change the outcome.

The expansion of the free energy, Eq. (2.43) in powers of m and Δ yields

$$\mathcal{F}=\alpha_\Delta\Delta^2+\alpha_m m^2+A\Delta^4+Bm^4+2C\Delta^2m^2. \tag{5.1}$$

where $\mathcal{F}=\Delta F(m,\Delta)/(4N_F)$. Coefficients α_Δ, α_m, A, and B in Eq. (5.1) are identical for both s^{+-} and s^{++} SC states:

$$\alpha_\Delta=\frac{1}{2}\ln\frac{T}{T_c}, \tag{5.2}$$

$$\alpha_m=\frac{1}{2}\left(\ln\frac{T}{T_s}+2\pi T\sum_{\varepsilon_n>0}\left\langle\frac{\delta_{\hat{\mathbf{k}}}^2}{\varepsilon_n(\varepsilon_n^2+\delta_{\hat{\mathbf{k}}}^2)}\right\rangle\right) \tag{5.3}$$

and

$$A=\frac{\pi T}{4}\sum_{\varepsilon_n>0}\frac{1}{\varepsilon_n^3}, \tag{5.4}$$

$$B=\frac{\pi T}{4}\sum_{\varepsilon_n>0}\left\langle\varepsilon_n\frac{\varepsilon_n^2-3\delta_{\hat{\mathbf{k}}}^2}{(\varepsilon_n^2+\delta_{\hat{\mathbf{k}}}^2)^3}\right\rangle. \tag{5.5}$$

The difference between s^{+-} and s^{++} SC orders appears only in the coefficient C. For s^{+-} state we have

$$C_{(+-)}=\frac{\pi T}{4}\sum_{\varepsilon_n>0}\left\langle\frac{\varepsilon_n^2-\delta_{\hat{\mathbf{k}}}^2}{\varepsilon_n(\varepsilon_n^2+\delta_{\hat{\mathbf{k}}}^2)^2}\right\rangle \tag{5.6}$$

while for s^{++}

$$C_{(++)}=\frac{\pi T}{4}\sum_{\varepsilon_n>0}\left\langle\frac{3\varepsilon_n^2+\delta_{\hat{\mathbf{k}}}^2}{\varepsilon_n(\varepsilon_n^2+\delta_{\hat{\mathbf{k}}}^2)^2}\right\rangle. \tag{5.7}$$

Note that, although both C coefficients are positive, this does not preclude coexistence in Eq. (5.1), and we find below that the sign of parameter $\chi=AB-C^2$ is more important for coexistence. We will demonstrate that since $C_{(++)}>C_{(+-)}$, χ is positive for a broader range of parameters in s^{+-} state than that in s^{++} state. In fact, χ remains always negative in s^{++} state. Below we will use the notion that $\chi>0$ corresponds to an effective attraction between the two orders.

The free energy, Eq. (5.1), has two local minima, corresponding to pure states, when one of the order parameters is identically equal to zero.

(1) A pure SC state, defined by $m=0$ and $\partial\mathcal{F}/\partial\Delta=0$, has the free energy and SC order parameter

$$\mathcal{F}_\Delta = -\frac{\alpha_\Delta^2}{4A}, \quad \Delta^2 = -\frac{\alpha_\Delta}{2A}, \tag{5.8}$$

(2) a pure SDW state, defined by $\Delta=0$ and $\partial\mathcal{F}/\partial m=0$, has the free energy and SDW order parameter

$$\mathcal{F}_m = -\frac{\alpha_m^2}{4B}, \quad m^2 = -\frac{\alpha_m}{2B}. \tag{5.9}$$

In addition, the free energy may also have either a saddle point or a global minimum when both $\Delta\neq 0$ and $m\neq 0$. To see this, we write the free energy Eq. (5.1) in equivalent form

$$\mathcal{F} = \alpha_m\left(m^2+\frac{C}{B}\Delta^2\right)+B\left(m^2+\frac{C}{B}\Delta^2\right)^2+\left(\alpha_\Delta-\frac{C}{B}\alpha_m\right)\Delta^2 + \left(A-\frac{C^2}{B}\right)\Delta^4,$$

which is now a sum of two independent parts for Δ^2 and $M^2\equiv m^2+(C/B)\Delta^2$. For an extremum state, given by $\partial_\Delta\mathcal{F}=\partial_m\mathcal{F}=0$, the stationary values of order parameters,

$$\Delta^2 = -\frac{\alpha_\Delta B-\alpha_m C}{2(AB-C^2)}, \quad M^2 = m^2+\frac{C}{B}\Delta^2 = -\frac{\alpha_m}{2B}, \tag{5.10}$$

determine the free energy,

$$\mathcal{F}_{m\&\Delta} = -BM^4-\frac{AB-C^2}{B}\Delta^4. \tag{5.11}$$

When both coefficients in Eq. (5.11) are positive,

$$B>0, \quad \chi = AB-C^2>0, \tag{5.12}$$

the mixed state, Eq. (5.10), corresponds to the minimum of the free energy, which is smaller than the minima for pure SC or SDW states,

$$\mathcal{F}_{m\&\Delta} = \mathcal{F}_m-\frac{1}{4B}\frac{(\alpha_\Delta B-\alpha_m C)^2}{AB-C^2} = \mathcal{F}_\Delta-\frac{1}{4A}\frac{(\alpha_m A-\alpha_\Delta C)^2}{AB-C^2}. \tag{5.13}$$

Consequently, in the phase diagram, the pure SDW and SC states are separated by a SDW+SC phase and the transitions into this intermediate state are second order. However, if $B>0$ and $\chi<0$, the mixed phase, Eq. (5.10), corresponds to the saddle point of the free energy and is not thermodynamically stable phase. In this case, pure SDW and SC phases are separated by a first-order transition line. When $B<0$, one needs to expand further in m to determine the phase diagram. We will not discuss the case $B<0$ further within GL theory.

We apply Eq. (5.12) to the case $\delta_{\hat{\mathbf{k}}}=\delta_0+\delta_2\cos 2\phi$ which we considered in the previous sections. We remind that $\delta_2=0$ corresponds to cocircular FSs with different chemical potentials while $\delta_0=0$ corresponds to FS geometry in which $k_F^c=k_F^f$ but the electron pocket is elliptical.

At perfect nesting $\delta_0=\delta_2=0$ and the system develops an SDW order at $T_s>T_c$. Deviations from perfect nesting lead to two effects. First, as we already said, the magnitude of α_m is reduced because SDW instability is suppressed when nesting becomes nonperfect. Superconducting α_Δ is not affected by $\delta_{\hat{\mathbf{k}}}$ and eventually wins over SDW. Second, coefficients B and C evolve with $\delta_{\hat{\mathbf{k}}}$ and, as a result, the sign of $\chi=AB-C^2$ depends on values of δ_0 and δ_2.

The GL expansion is applicable only in the vicinity of points at which the temperatures of the SDW-N and SC-N transitions coincide $T_s(\delta_{\hat{\mathbf{k}}})=T_c$. This condition together with Eq. (3.6) establish the relation between δ_0 and δ_2 at which one needs to compute the parameters B and C.

1. s^{+-} superconductivity

To get an insight on how χ evolves with $\delta_{\hat{\mathbf{k}}\mathbf{q}}$, we first assume that T_s/T_c is only slightly larger than one ($T_s/T_c=1+\delta t$), in which case $T_s(\delta_{\hat{\mathbf{k}}})=T_c$ at small δ_0 and δ_2, and we can expand A, B, and C in powers of δ_0 and δ_2. Specifically, we have from Eq. (3.6),

$$\delta t = \frac{7\zeta(3)}{4\pi^2T_s^2}\left(\delta_0^2+\frac{1}{2}\delta_2^2\right) = \frac{0.663}{m_0^2}\left(\delta_0^2+\frac{1}{2}\delta_2^2\right), \tag{5.14}$$

where $\zeta(3)$ is a Riemann-Zeta function. Collecting terms up to the fourth order in the expansion, we obtain

$$\chi = \frac{1}{32\pi^8T_c^8}(s_1\langle\delta_{\hat{\mathbf{k}}}^4\rangle-s_2\langle\delta_{\hat{\mathbf{k}}}^2\rangle^2), \tag{5.15}$$

where

$$s_1 = 5\left(\sum_{n\geq 0}\frac{1}{(2n+1)^3}\right)\left(\sum_{n\geq 0}\frac{1}{(2n+1)^7}\right), \quad s_2 = 9\left(\sum_{n\geq 0}\frac{1}{(2n+1)^5}\right)^2. \tag{5.16}$$

The sums are expressed in terms of the Riemann-Zeta function $\zeta(3)$, $\zeta(5)$, and $\zeta(7)$ and give $s_1\approx 5.261$ and $s_2\approx 9.082$. Substituting $\delta_{\hat{\mathbf{k}}}=\delta_0+\delta_2\cos 2\phi$ and averaging over momentum direction ϕ on the FSs, we obtain

$$\chi \approx \frac{1}{32\pi^8T_c^8}(-3.820\delta_0^4+6.703\delta_0^2\delta_2^2-0.297\delta_2^4). \tag{5.17}$$

We see that for $\delta_0=\delta_2=0$, $\chi=0$, i.e., for a perfect nesting the system cannot distinguish between first-order transition and SDW+SC phase. This result, first noticed in Ref. 29, implies that the phase diagram is quite sensitive to the interplay between δ_0 and δ_2. We see from Eq. (5.17) that in the two limits when either $\delta_2=0$ or $\delta_0=0$, $\chi<0$, i.e., the transition is first order. This agrees with the numerical analysis in the previous section. We emphasize that in both limits, a small SDW order, which we consider here, still preserves low-energy fermionic states near the modified FSs. Fermions near these FSs do have a possibility to pair into s^{+-} state. However, SDW+SC state turns out to be energetically unfavorable. We particularly emphasize that the ellipticity of electron dispersion is not sufficient for the appearance of the SDW+SC phase near $T_c\sim T_s$.

When both $\delta_0\neq 0$ *and* $\delta_2\neq 0$, there is a broad range

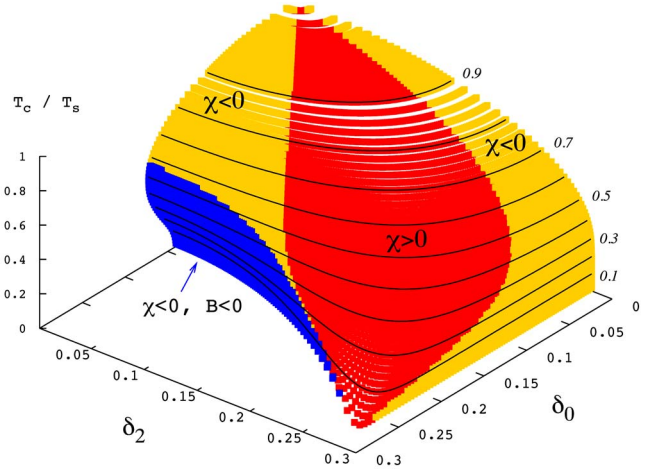

FIG. 15. (Color online) The three-dimensional plot of the SDW-SC crossing surface, $T_s(\delta_0,\delta_2)=T_c$. At each point on the surface we show the sign of B and $\chi=AB-C^2$. In the region where $\chi>0$, the transition between SDW and SC states occurs via the coexistence region. For $\chi<0$, pure SDW and SC states are separated by the first-order transition. When $B<0$, the SDW-N conversion is of the first order and the present GL analysis is invalid.

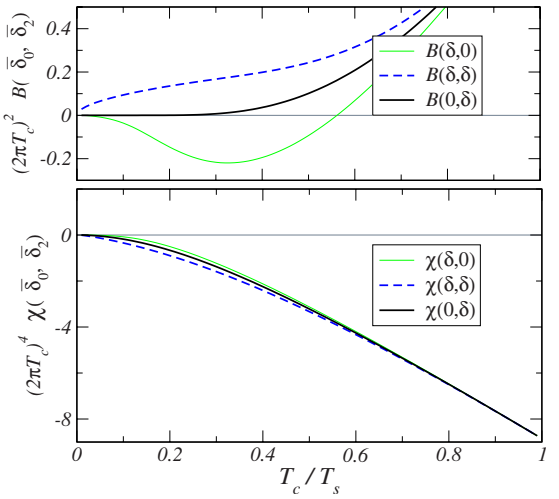

FIG. 16. (Color online) The case of s^{++} SC. Panel (a): the behavior of $\chi(\delta_0,\delta_2)=AB-C^2$ for different T_s/T_c for three cases: $\chi(\delta,0)$, $\chi(0,\delta)$, and $\chi(\delta,\delta)$. For each case, δ is chosen to satisfy the condition $T_s(\delta_0,\delta_2)=T_c$ for a given T_s/T_c. We see that in all three cases, $\chi<0$ no matter what the ration T_s/T_c is. Panel (b): the coefficient $B(\delta_0,\delta_2)$ along the line $T_s(\delta_0,\delta_2)=T_c$. GL analysis is only valid when $B>0$.

$$0.765 < \frac{\delta_2}{\delta_0} < 4.689, \tag{5.18}$$

where $\chi>0$ and the transition from a pure SDW phase to pure a SC phase occurs via an intermediate phase where the two orders coexist. This also agrees with the numerical analysis (see Figs. 8 and 10).

Equation (5.18) has to be combined with the equation for $T_s(\delta_0,\delta_2)=T_c$, and the boundaries in Eq. (5.18) set the critical values of δ_2 and δ_0 as functions of T_s/T_c. Combining Eqs. (5.18) and (5.14), we obtain that coexistence occurs for

$$0.826 m_0\sqrt{\delta t} < \delta_2 < 1.663 m_0\sqrt{\delta t}. \tag{5.19}$$

To verify that this result holds at larger values of δ_0 and δ_2, we computed χ without expanding in $\delta_{\hat{\mathbf{kq}}}$. We plot the resulting phase diagram in Fig. 15. The result is qualitatively the same as Eq. (5.17): for $\delta_0=0$ or $\delta_2=0$, $\chi<0$ and the transition between SDW and SC states is of first order while when both δ_0 and δ_2 are nonzero, there exists a region where $\chi>0$ and the transition from SDW to SC state occurs via an intermediate SDW+SC phase.

2. s^{++} superconductivity

We performed the same calculations for a conventional, sign-preserving s-wave superconductivity. The key difference with the s^{+-} case is that now $\chi=AB-C^2$ is nonzero already when $\delta_0=\delta_2=0$. Substituting A and B from Eqs. (5.4) and (5.5) and C from Eq. (5.7) we obtain

$$\chi(\delta_{\hat{\mathbf{kq}}}=0) = -\frac{7\zeta(3)}{128\pi^4 T_c^4} < 0. \tag{5.20}$$

The implication is that, for small δ_0 and δ_2, χ remains negative and the transition between SDW and SC states is first order. This result was first obtained by Fernandes *et al.* in Ref. 29. These authors also argued, based on their numerical analysis of the free energy, that there is no SDW+SC phase for s^{++} gap even when $\delta_0=\delta_2$ are not small. We analyzed the sign of χ for larger δ_0 and δ_2 using our analytical formulas and confirmed their result. In Fig. 16 we show the behavior of $\chi(\delta_0,\delta_2)$ at the transition point $T_s(\delta_0,\delta_2)=T_c$ for three representative cases: $\chi(\delta_0,0)$, $\chi(0,\delta_2)$, and $\chi(\delta_0,\delta_2=\delta_0)$. In all cases, when $B>0$ (e.g., our GL analysis is valid) $\chi(\delta_0,\delta_2)$ remains negative.

We caution, however, that the absence of coexistence between s^{++} SC and SDW states within GL model does not imply that the two states are always separated by first-order transition. GL analysis is only valid near $T_s(\delta_0,\delta_2)=T_c$, when both orders are weak. The situation at lower T has to be analyzed without expanding in m and Δ. And, indeed, we did find a small coexistence region $T=0$, see Fig. 14.

B. Zero-temperature limit

We consider only the case of $s^{\pm}$ SC and the limit when relevant δ_0 and δ_2 are small, i.e., when $T_s/T_c=1+\delta t$ and $\delta t \ll 1$. We compare energies for pure SDW and SC state and for the coexistence state and find the region where the coexistence state is energetically favorable.

For this, we first verified that, at small δ_0 and δ_2, the values of SDW and SC order parameters at $T=0$ remain the same as at $\delta_2=\delta_0=0$, i.e., $m=m_0=0.28073\times(2\pi T_s)$ and $\Delta=\Delta_0=m_0(T_c/T_s)$. These values only change at large enough δ_0 and δ_2, e.g., m changes when $\delta_0+\delta_2>m_0$.

The free energies of pure SDW and SC states for $m,\Delta>\delta_0+\delta_2$ can be straightforwardly evaluated at $T=0$ by replacing the frequency sums in Eq. (2.43) by integrals. We obtain

$$\mathcal{F}(m) = -\frac{m^2}{4} + \frac{\delta_0^2}{2} + \frac{\delta_2^2}{4} + \frac{m^2}{2}\ln\frac{m}{m_0}, \tag{5.21}$$

$$\mathcal{F}(\Delta) = -\frac{\Delta^2}{4} + \frac{\Delta^2}{2}\ln\left(\frac{\Delta}{\Delta_0}\right). \tag{5.22}$$

These free energies have minima at $m=m_0$ and $\Delta=\Delta_0$, respectively. At the minima,

$$\mathcal{F}(m_0) = -\frac{m_0^2}{4} + \frac{\delta_0^2}{2} + \frac{\delta_2^2}{4},$$

$$\mathcal{F}(\Delta_0) = -\frac{\Delta_0^2}{4} = -\left(\frac{T_c}{T_s}\right)^2 \frac{m_0^2}{4}. \tag{5.23}$$

Observe that $\mathcal{F}(\Delta_0) < \mathcal{F}(m_0)$ when $T_c = T_s$. This is the consequence of the fact that SDW magnetism is destroyed by doping and ellipticity while superconductivity is unaffected.

Comparing $\mathcal{F}(m_0)$ and $\mathcal{F}(\Delta_0)$, we find that the first-order transition between pure SDW and SC states occurs at

$$m_0^2 \delta t = \delta_0^2 + \delta_2^2/2. \tag{5.24}$$

If there is no intermediate coexistence phase, the SDW state is stable for $\delta_0 \leq \sqrt{m_0^2 \delta t - \delta_2^2/2}$ while SC state is stable for larger values of δ_0.

We next determine when the intermediate state appears at $T=0$. For this we expand the free energy near the SDW and SC states in powers of Δ and m, respectively. We obtain near the SDW state,

$$\mathcal{F}(m,\Delta) = \mathcal{F}(m_0) + a_\Delta \Delta^2 + b_\Delta \Delta^4 \tag{5.25}$$

and near the SC state

$$\mathcal{F}(m,\Delta) = \mathcal{F}(\Delta_0) + a_m m^2 + b_m m^4. \tag{5.26}$$

We verified that b_Δ and b_m are positive while a_m and a_Δ can be of either sign. The key issue is what are the signs of a_m and a_Δ at the point where $\mathcal{F}(m_0)=\mathcal{F}(\Delta_0)$. We found that, to leading order in δt, $a_m = a_\Delta = a$ at this point and a is given by

$$a = \frac{\delta t^2}{6}(1 - 8z + 7z^2), \quad z = \frac{\delta_2^2}{2m_0^2 \delta t}. \tag{5.27}$$

Note that to obtain a we had to expand to order δt^2. By virtue of Eq. (5.24), $\delta_0 = m_0\sqrt{\delta t}\sqrt{1-z}$, i.e., we have to consider $z \leq 1$.

When a is positive, both pure states are stable and there is a first-order transition between them. When $a<0$, the pure SDW and SC states are already unstable at the point where $\mathcal{F}(m_0)=\mathcal{F}(\Delta_0)$, what implies that when we vary δ_0 at a fixed δ_2, there is a range of δ_0 around $\delta_0 = m_0\sqrt{\delta t}\sqrt{1-z}$ in which the coexistence state has a lower energy than the pure states. From Eq. (3.1) we see that $a>0$ when $z<1/7$ while $a<0$ for $1/7<z<1$. In terms of δ_2, this implies that the transition at $T=0$ is first order between pure states when $\delta_2 < 0.535 m_0\sqrt{\delta t}$ while at larger δ_2, pure SDW and SC phases are separated along δ_0 line by the region of the coexistence phase. The width of the coexistence phase initially increases as δ_2 increases but then begins to shrink and vanishes when δ_2 approaches $\delta_2 = 1.414 m_0\sqrt{\delta t}$ (z approaches one from below). At this point, the coexistence region shrinks to a point $\delta_0=0$. At larger δ_2, the SC state has lower energy than the SDW state for all values of δ_0.

If we keep δ_0 fixed but vary δ_2, the coexistence range appears at $\delta_0=+0$ ($z=1$) and exists up to $\delta_0 = 0.926 m_0\sqrt{\delta t}$ ($z=1/7$). At larger δ_0 ($z<1/7$), there is a first-order transition between pure SDW and SC states.

C. Phase diagram

We now combine the results of GL analysis near the crossing point and at $T=0$ into the phase diagrams. For definiteness, we set $\delta t = T_s/T_c - 1$ to be small and consider the set of phase diagrams in variables T and δ_0 for different fixed δ_2. The results of this section has to be compared with the phase diagrams presented in panels (a1)–(a3) in Fig. 7, see also Fig. 10.

From the analysis in the preceding two sections, we found five critical values of δ_2: two are obtained from the GL analysis of the range of the coexistence phase, and are given by Eq. (5.19), two are critical values at which the coexistence phase first appears and then disappears at $T=0$, and the last one is the maximum value of δ_2 at which $T_s(\delta_0=0,\delta_2) = T_c$. From Eq. (5.14) this value is $\delta_2 = 1.739 m_0\sqrt{\delta t}$. Arranging these five values from the smallest to the largest, we obtain the following set of phase diagrams at small δt.

(a) For $\delta_2 < 0.535 m_0\sqrt{\delta t}$, there is no intermediate phase, and pure SDW and SC transitions are separated by a line of a first-order transition. The line is tilted toward smaller δ_0 at smaller T: it originates at $\delta_0 = m_0\sqrt{\delta t}[1.508 - 0.5\delta_2^2/(m_0^2\delta t)]^{1/2}$ at $T=T_c$ and ends up at $\delta_0 = m_0\sqrt{\delta t}[1 - 0.5\delta_2^2/(m_0^2\delta t)]^{1/2}$.

(b) For $0.535 m_0\sqrt{\delta t} < \delta_2 < 0.826 m_0\sqrt{\delta t}$, the intermediate phase appears near $T=0$ and extends to some $T<T_c$. At larger T, the transition remains first order. This behavior is consistent with the panel (a1) in Fig. 7.

(c) For $0.826 m_0\sqrt{\delta t} < \delta_2 < 1.414 m_0\sqrt{\delta t}$, the intermediate phase occupies the whole region $T<T_c$. This behavior is consistent with the panel (a2) in Fig. 7.

(d) For $1.414 m_0\sqrt{\delta t} < \delta_2 < 1.663 m_0\sqrt{\delta t}$, SC state wins at $T=0$ for all δ_0. There is phase transition at finite T. The transition is first order between pure SDW and SC state at smaller T but the coexistence phase still survives near T_c. This behavior is consistent with the panel (a3) in Fig. 7.

(e) For $1.663 m_0\sqrt{\delta t} < \delta_2 < 1.739 m_0\sqrt{\delta t}$, the coexistence phase near T_c disappears and the transition becomes first order along the whole line separating SDW and SC states.

(f) For $\delta_2 > 1.739 m_0\sqrt{\delta t}$, $T_s(\delta_0,\delta_2)$ becomes smaller than T_c for all δ_0 and the system only develops a SC order.

This behavior is also totally consistent with Fig. 10: all different phase diagrams are reproduced if we take horizontal cuts at different δ_2. We see therefore that numerical and analytical analysis is in full agreement with each other.

The only result of numerical studies not reproduced in small δt analytical expansion is the existence of a range of δ_2 where the transition between the SDW phase and the coexistence phase is second order while the transition between the SC phase and the coexistence phase is first order, see Fig. 10. To reproduce this effect in analytical treatment, we would have to expand to the next order in δt. Note in this regard that it is evident from Fig. 10 that the width of the range where one transition is first order and another is second order shrinks as T_s/T_c decreases.

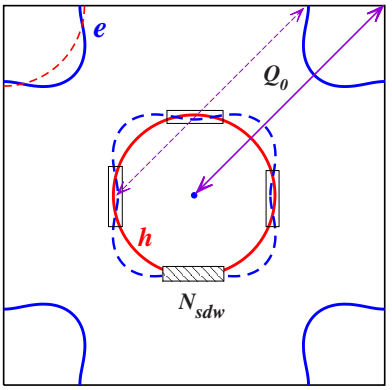

FIG. 17. (Color online) A partially gapped SDW state, where only a fraction N_{SDW} of the electron and hole FSs is nested. On the remaining parts the dispersions ξ_f and ξ_c are very different. The SDW state appearing below T_s gaps excitations only in the shaded/boxed areas [see Fig. 2(d)] while on the rest of the FSs the dispersions are close to the original ξ_f and ξ_c. The SC state below T_c does not compete with SDW in non-nested regions but competes with SDW state in the nested (boxed) regions.

VI. PARTIAL SDW STATE

In previous sections we considered the situation when the splitting between hole and electron FSs is small. We now consider how the phase diagram is modified if in some k-regions hole and electron FSs are quite apart from each other (after we shift the hole FS by $\mathbf{Q}_0$). Such regions are far from nesting and we make a simple assumption that they are not affected by SDW. We then split the FS into nested parts where commensurate SDW state exists and a SC order can exist as well, and non-nested parts, where only SC order is possible. We present this schematically in Fig. 17. The nested parts lie in some intervals of angles ϕ with total circumference $\Delta\phi$ and have weight $N_{SDW}<N_{total}=1$ ($\Delta\phi/2\pi=N_{SDW}/N_{total}$).

The free energy and the self-consistency equations then can be written as sums of the two contributions. The first sum is over the FS part that has only SC order parameter and in the second sum we integrate over part of the FS with both orders,[37]

$$\frac{\Delta F(\Delta,m)}{4N_F} = \frac{\Delta^2}{2}\ln\frac{T}{T_c} + N_{SDW}\frac{m^2}{2}\ln\frac{T}{T_s} - 2\pi T\sum_{\varepsilon_n>0}(1-N_{SDW})\left[\sqrt{\varepsilon_n^2+\Delta^2}-|\varepsilon_n|-\frac{\Delta^2}{2|\varepsilon_n|}\right] - 2\pi T\sum_{\varepsilon_n>0}\int_{\Delta\phi}\frac{d\phi}{2\pi} \times \mathrm{Re}\left[\frac{1}{2}(\Sigma_+ + \Sigma_-) - |\varepsilon_n| - \frac{\Delta^2}{2|\varepsilon_n|} - \frac{m^2}{2|\varepsilon_n|}\right], \quad (6.1)$$

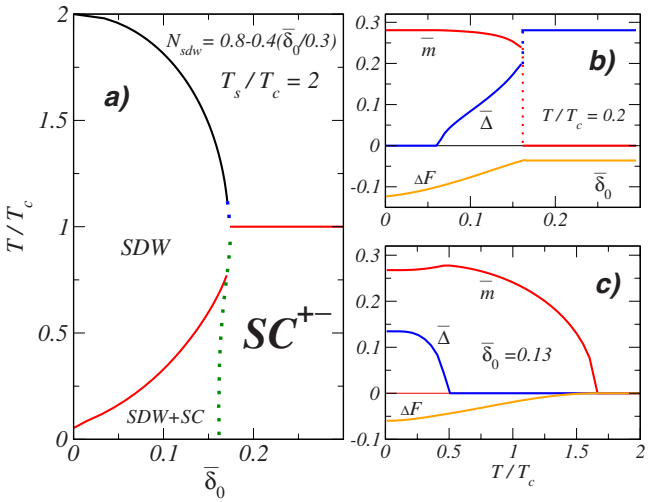

FIG. 18. (Color online) (a) The phase diagram for s^{+-} superconductivity and SDW order parameter existing only in boxed regions of the FS in Fig. 17, with the relative width N_{SDW}. We manually set the doping dependence of N_{SDW} to be $N_{SDW}=0.8-0.4(\bar{\delta}_0/0.3)$ and neglected the effect of this variation in N_{SDW} on T_s. Observe that SC and SDW orders coexist in a wide range of δ_0 and T. [(b)and (c)] the order parameters, Δ and m, and the free energy, F, as functions of δ_0 at a constant temperature, $T/T_c=0.2$ (b) and as functions of T at a constant $\bar{\delta}_0=0.13$ (c). As a function of δ_0, SDW order parameter starts decreasing when SC order appears and then jumps to zero and the system becomes a pure SC.

$$\Delta\ln\frac{T}{T_c} = 2\pi T\sum_{\varepsilon_n>0}(1-N_{SDW})\left[\frac{\Delta}{\sqrt{\varepsilon_n^2+\Delta^2}}-\frac{\Delta}{|\varepsilon_n|}\right] + 2\pi T\sum_{\varepsilon_n>0}\int_{\Delta\phi}\frac{d\phi}{2\pi}\mathrm{Re}\left[\frac{1}{2}\left(\frac{\partial\Sigma_+}{\partial\Delta}+\frac{\partial\Sigma_-}{\partial\Delta}\right)-\frac{\Delta}{|\varepsilon_n|}\right], \quad (6.2)$$

$$N_{SDW}m\ln\frac{T}{T_s} = 2\pi T\sum_{\varepsilon_n>0}\int_{\Delta\phi}\frac{d\phi}{2\pi}\mathrm{Re}\left[\frac{1}{2}\left(\frac{\partial\Sigma_+}{\partial m}+\frac{\partial\Sigma_-}{\partial m}\right)-\frac{m}{|\varepsilon_n|}\right]. \quad (6.3)$$

The self-consistency Eqs. (6.2) and (6.3) are obtained by minimization of the functional ΔF, $\partial(\Delta F)/\partial\Delta=0$ and $\partial F/\partial m=0$, and these expressions reduce to previous formulas (2.41)–(2.43) for $N_{SDW}=1$.

We find that the results are very similar to what we found within the approximation of a small FS splitting. The typical picture is shown in Fig. 18.

The only differences from Fig. 8 in this case are the coexistence of SC and SDW states already at zero doping $\delta_0=0$ and weak first-order transition to purely SC state. We also analyzed s^{++} SC order and again found a much weaker tendency for co-existence, similar to Fig. 14.

VII. CONCLUSIONS

To conclude, we presented a general theoretical description of the interplay between itinerant SDW and SC orders in

two-band metals. Within the mean-field approach we derived coupled self-consistency equations for the order parameters and the expression for the free energy, which is necessary to determine the stability of different phases.

We considered the FS geometry with one-hole and one-electron bands of different shapes (a simplified FS geometry for Fe pnictides) and investigated the phase diagrams and the stability of the SDW+SC states for: (a) different gap structures of the SC state, Figs. 8 and 10 vs Fig. 14; (b) variations in the relative strength of SDW and SC interactions, Figs. 10 and 11; (c) ellipticity of electron pockets, Figs. 7, 8, and 10; and (d) incommensuration of SDW order, Figs. 11 and 12. We considered the case when the transition temperature to pure SDW state, T_s, is higher than the critical temperature T_c of a pure SC state. In the opposite case, $T_s < T_c$, the SC state develops first and suppresses SDW state.

We found that the SC $s^{\pm}$ state with extended s-wave symmetry has much stronger affinity with the SDW state than the traditional s^{++} state. A coexistence region of s^{++} SC state with SDW is tiny and the coexistence is anyway very weak in terms of energy gain compared to the pure SDW state. The transition from the pure SDW state to the pure SC state is always first order, Fig. 14. For $s^{\pm}$ gap, there is a stronger inclination toward coexistence with SDW state due to effective attraction between the two orders. We found that, depending on the interplay between different effects (e.g., ellipticity and doping), the transition between SDW and SC orders is either first order or continuous, via the intermediate SDW+SC phase, in which both order parameters are nonzero, Figs. 6–8.[63]

We note that the coexistence region gets larger with increased strength of the SDW interaction relative to its SC counterpart, described by the ratio T_s/T_c. Thus generally we should see better coexistence between SDW and SC states, if T_s is increasingly larger than T_c, Fig. 10.

Our results are in a disagreement with a common belief that, because SDW and SC states compete for the Fermi surface, the SDW+SC state should emerge when a pure SDW state next to the boundary of the coexistence region still has a modified Fermi surface at $T=0$ and should not emerge when fermionic excitations in the pure SDW phase are fully gapped at zero temperature. We found that the key reason for the existence of the mixed SDW+SC state is the "effective attraction" between the SDW and SC orders while the presence or absence of the Fermi surface in the SDW state at $T=0$ matters less. Specifically, we found cases when SDW and SC orders do coexist even when fermionic excitations in the pure SDW phase are fully gapped at $T=0$, Fig. 10(a), and we also found, for s^{++} pairing, that there might be no coexistence down to $T=0$ even when the pure SDW phase has a Fermi surface, Fig. 14.

The phase diagrams for s^{+-} gap are quite consistent with the experimental findings in pnictides. For example, first-order transition in Fig. 6 looks very similar to phase diagram of 1111 materials (La,Sm)OFeAs, where FSs are more cylindrical. The coexistence region in Fig. 8 correlates well with doped 122 materials based on $BaFe_2As_2$, where hole and electron FSs are less nested. And Fig. 10 shows that one can get both SDW+SC phase and first-order transitions for the same SC state and the same family of materials. Our key result is that the way the doping is introduced into the sample will determine the nature of the FS changes and the path it will take in the (δ_0, δ_2) plane: whether through a first-order transition or through a coexistence region. In other words, we argue that there is strong correlation between how exactly FSs evolve upon doping and whether or not SC and SDW states coexist.

The final remark. In the literature, there exists a notion of "homogeneous" and "inhomogeneous" coexistence of SC and SDW orders. The latter is a metastable state when the two orders exist in *different* spatial parts of the material. What we emphasize is that the other kind, homogeneous coexistence of SC and SDW orders in real space, is in fact inhomogeneous in momentum space: the SC and SDW orders dominate excitation gaps on different parts of the FS.

ACKNOWLEDGMENTS

We acknowledge with thanks useful discussions with D. Agterberg, V. Cvetkovic, R. Fernandes, I. Eremin, I. Mazin, J. Schmalian, O. Sushkov, and Z. Tesanovic. The work was supported by NSF Grants No. DMR-0906953 (A.V.C.) and No. DMR-0955500 (M.G.V.).

APPENDIX: ELECTRON AND HOLE DISPERSION FOR SMALL FS SPLITTING

In this appendix, we discuss in detail the approximation we used for the dispersions of holes and electrons for the case when the splitting between hole and electron FSs is small.

SDW and SC orders mix c fermions with momenta $\mathbf{k}$ and f fermions with momenta $\mathbf{k}+\mathbf{q}$. The generic expressions for the two dispersions are

$$\xi_c(\mathbf{k}) = \mu_c - \frac{(\mathbf{k})^2}{2m_c}, \quad \xi_f(\mathbf{k}+\mathbf{q}) = \frac{(k+q)_x^2}{2m_{fx}} + \frac{(k+q)_y^2}{2m_{fy}} - \mu_f. \tag{A1}$$

When the two FSs are circles of nonequal size, $m_{fx}=m_{fy}=m_f$, we have $(\mu_c, m_c) \approx (\mu_f, m_f) \approx (\mu, m)$ but $m_c \neq m_f$ and $\mu_c \neq \mu_f$. The approximation we used in the text implies that

$$\xi_c(\mathbf{k}) = \mu_c - \frac{(k+q)^2}{2m_c} = \frac{\mu_c+\mu_f}{2} - \frac{k^2}{4}\left(\frac{1}{m_c}+\frac{1}{m_f}\right) - \frac{\mathbf{kq}}{4}\left(\frac{1}{m_c}+\frac{1}{m_f}\right) + \frac{\mu_c-\mu_f}{2} - \frac{k^2}{4}\left(\frac{1}{m_c}-\frac{1}{m_f}\right) + \frac{\mathbf{kq}}{4}\left(\frac{1}{m_c}+\frac{1}{m_f}\right)$$
$$\approx \frac{\mu_c+\mu_f}{2} - \frac{k^2}{4}\left(\frac{1}{m_c}+\frac{1}{m_f}\right) - \frac{\mathbf{kq}}{4}\left(\frac{1}{m_c}+\frac{1}{m_f}\right) + \frac{\mu_c-\mu_f}{2} + \frac{k_F^2}{4m}(m_c-m_f) + \frac{\mathbf{k}_F\mathbf{q}}{2m}$$

$$\xi_f(\mathbf{k}+\mathbf{q}) = \frac{(k+q)^2}{2m_f} - \mu_f = \frac{k^2}{4}\left(\frac{1}{m_c}+\frac{1}{m_f}\right) + \frac{\mathbf{kq}}{4}\left(\frac{1}{m_c}+\frac{1}{m_f}\right) - \frac{\mu_c+\mu_f}{2} + \frac{\mu_c-\mu_f}{2} - \frac{k^2}{4}\left(\frac{1}{m_c}-\frac{1}{m_f}\right) + \frac{\mathbf{kq}}{4}\left(\frac{3}{m_f}-\frac{1}{m_c}\right)$$
$$\approx \frac{k^2}{4}\left(\frac{1}{m_c}+\frac{1}{m_f}\right) + \frac{\mathbf{kq}}{4}\left(\frac{1}{m_c}+\frac{1}{m_f}\right) - \frac{\mu_c+\mu_f}{2} + \frac{\mu_c-\mu_f}{2} + \frac{k_F^2}{4m}(m_c-m_f) + \frac{\mathbf{k}_F\mathbf{q}}{2m} \quad \text{(A2)}$$

Introducing $\xi_{\mathbf{kq}}$ and $\delta_{\hat{\mathbf{kq}}}$ defined in Eq. (2.30), we obtain

$$\xi_{\mathbf{kq}} = \frac{k^2}{4}\left(\frac{1}{m_c}+\frac{1}{m_f}\right) + \frac{\mathbf{kq}}{4}\left(\frac{1}{m_c}+\frac{1}{m_f}\right) - \frac{\mu_c+\mu_f}{2},$$

$$\delta_{\hat{\mathbf{kq}}} = \frac{\mu_c-\mu_f}{2} + \frac{k_F^2}{4m}(m_c-m_f) + \frac{\mathbf{k}_F\mathbf{q}}{2m} = \frac{1}{2}\mathbf{v}_F(\mathbf{k}_F^c - \mathbf{k}_F^f - \mathbf{q}). \quad \text{(A3)}$$

We emphasize that, within this approximation, $\xi_{\mathbf{kq}}$ and $\delta_{\hat{\mathbf{kq}}}$ are two independent variables, one depends on the deviation along the FS in the transverse direction and another depends on the angle along the FS. When $m_{fx} \neq m_{fy}$, the derivation remains the same but $\delta_{\hat{\mathbf{kq}}}$ acquires an additional term with the difference between m_{fx} and m_{fy} (the $\cos 2\phi$ term).

[1] Y. Kamihara, T. Watanabe, M. Hirano, and H. Hosono, J. Am. Chem. Soc. **130**, 3296 (2008).
[2] M. Rotter, M. Tegel, and D. Johrendt, Phys. Rev. Lett. **101**, 107006 (2008).
[3] F.-C. Hsu, J.-Y. Luo, K.-W. Yeh, T.-K. Chen, T.-W. Huang, P. M. Wu, Y.-C. Lee, Y.-L. Huang, Y.-Y. Chu, D.-C. Yan, and M.-K. Wu, Proc. Natl. Acad. Sci. U.S.A. **105**, 14262 (2008).
[4] A. Subedi, L. Zhang, D. J. Singh, and M. H. Du, Phys. Rev. B **78**, 134514 (2008).
[5] L. Bulaevskii, A. Buzdin, M. Kulic, and S. Panjukov, Adv. Phys. **34**, 175 (1985).
[6] Y. Ōnuki, R. Settai, K. Sugiyama, T. Takeuchi, T. C. Kobayashi, Y. Haga, and E. Yamamoto, J. Phys. Soc. Jpn. **73**, 769 (2004).
[7] F. Steglich, Physica C **460-462**, 7 (2007).
[8] D. H. Lu, M. Yi, S.-K. Mo, A. S. Erickson, J. Analytis, J.-H. Chu, D. J. Singh, Z. Hussain, T. H. Geballe, I. R. Fisher, and Z.-X. Shen, Nature (London) **455**, 81 (2008).
[9] D. H. Lu, M. Yi, S.-K. Mo, J. G. Analytis, J.-H. Chu, A. S. Erickson, D. J. Singh, Z. Hussain, T. H. Geballe, I. R. Fisher, and Z.-X. Shen, Physica C **469**, 452 (2009).
[10] C. Liu, G. D. Samolyuk, Y. Lee, N. Ni, T. Kondo, A. F. Santander-Syro, S. L. Bud'ko, J. L. McChesney, E. Rotenberg, T. Valla, A. V. Fedorov, P. C. Canfield, B. N. Harmon, and A. Kaminski, Phys. Rev. Lett. **101**, 177005 (2008).
[11] M. Yi, D. H. Lu, J. G. Analytis, J.-H. Chu, S.-K. Mo, R.-H. He, R. G. Moore, X. J. Zhou, G. F. Chen, J. L. Luo, N. L. Wang, Z. Hussian, D. J. Singh, I. R. Fisher, and Z.-X. Shen, Phys. Rev. B **80**, 024515 (2009).
[12] V. B. Zabolotnyy, D. S. Inosov, D. V. Evtushinsky, A. Koitzsch, A. A. Kordyuk, G. L. Sun, J. T. Park, D. Haug, V. Hinkov, A. V. Boris, C. T. Lin, M. Knupfer, A. N. Yaresko, B. Büchner, A. Varykhalov, R. Follath, and S. V. Borisenko, Nature (London) **457**, 569 (2009).
[13] A. V. Chubukov, D. V. Efremov, and I. Eremin, Phys. Rev. B **78**, 134512 (2008).
[14] A. V. Chubukov, Physica C **469**, 640 (2009).
[15] I. I. Mazin, D. J. Singh, M. D. Johannes, and M. H. Du, Phys. Rev. Lett. **101**, 057003 (2008).
[16] K. Kuroki, S. Onari, R. Arita, H. Usui, Y. Tanaka, H. Kontani, and H. Aoki, Phys. Rev. Lett. **101**, 087004 (2008).
[17] V. Barzykin and L. P. Gorkov, JETP Lett. **88**, 131 (2008).
[18] I. I. Mazin and J. Schmalian, Physica C **469**, 614 (2009).
[19] K. Seo, B. A. Bernevig, and J. Hu, Phys. Rev. Lett. **101**, 206404 (2008).
[20] T. A. Maier, S. Graser, D. J. Scalapino, and P. J. Hirschfeld, Phys. Rev. B **79**, 224510 (2009).
[21] S. Graser, T. A. Maier, P. J. Hirschfeld, and D. J. Scalapino, New J. Phys. **11**, 025016 (2009).
[22] A. V. Chubukov, M. G. Vavilov, and A. B. Vorontsov, Phys. Rev. B **80**, 140515(R) (2009).
[23] R. Thomale, C. Platt, J. Hu, C. Honerkamp, and B. A. Bernevig, Phys. Rev. B **80**, 180505(R) (2009).
[24] H. Luetkens, H.-H. Klauss, M. Kraken, F. J. Litterst, T. Dellmann, R. Klingeler, C. Hess, R. Khasanov, A. Amato, C. Baines, M. Kosmala, O. J. Schumann, M. Braden, J. Hamann-Borrero, N. Leps, A. Kondrat, G. Behr, J. Werner, and B. Büchner, Nature Mater. **8**, 305 (2009).
[25] S. Sanna, R. De Renzi, G. Lamura, C. Ferdeghini, A. Palenzona, M. Putti, M. Tropeano, and T. Shiroka, Phys. Rev. B **80**, 052503 (2009).
[26] Y. Laplace, J. Bobroff, F. Rullier-Albenque, D. Colson, and A. Forget, Phys. Rev. B **80**, 140501(R) (2009).
[27] M. H. Julien, H. Mayaffre, M. Horvatić, C. Berthier, X. D. Zhang, W. Wu, G. F. Chen, N. L. Wang, and J. L. Luo, EPL **87**, 37001 (2009).
[28] J.-H. Chu, J. G. Analytis, C. Kucharczyk, and I. R. Fisher, Phys. Rev. B **79**, 014506 (2009).
[29] R. Fernandes, D. Pratt, W. Tian, J. Zarestky, A. Kreyssig, S. Nandi, M. Kim, A. Thaler, N. Ni, P. Canfield, R. Mcqueeney, J. Schmalian, and A. Goldman, Phys. Rev. B **81**, 140501(R) (2010).
[30] H. Chen, Y. Ren, Y. Qiu, W. Bao, R. H. Liu, G. Wu, T. Wu, Y. L. Xie, X. F. Wang, Q. Huang, and X. H. Chen, EPL **85**, 17006 (2009).
[31] M. Rotter, M. Tegel, I. Schellenberg, F. M. Schappacher, R. Pöttgen, J. Deisenhofer, A. Günther, F. Schrettle, A. Loidl, and D.

Johrendt, New J. Phys. **11**, 025014 (2009).
[32] J. T. Park, D. S. Inosov, C. Niedermayer, G. L. Sun, D. Haug, N. B. Christensen, R. Dinnebier, A. V. Boris, A. J. Drew, L. Schulz, T. Shapoval, U. Wolff, V. Neu, X. Yang, C. T. Lin, B. Keimer, and V. Hinkov, Phys. Rev. Lett. **102**, 117006 (2009).
[33] T. Goko, A. A. Aczel, E. Baggio-Saitovitch, S. L. Bud'ko, P. C. Canfield, J. P. Carlo, G. F. Chen, P. Dai, A. C. Hamann, W. Z. Hu, H. Kageyama, G. M. Luke, J. L. Luo, B. Nachumi, N. Ni, D. Reznik, D. R. Sanchez-Candela, A. T. Savici, K. J. Sikes, N. L. Wang, C. R. Wiebe, T. J. Williams, T. Yamamoto, W. Yu, and Y. J. Uemura, Phys. Rev. B **80**, 024508 (2009).
[34] H. Shishido, A. Bangura, A. Coldea, S. Tonegawa, K. Hashimoto, S. Kasahara, P. Rourke, H. Ikeda, T. Terashima, R. Settai, Y. Onuki, D. Vignolles, C. Proust, B. Vignolle, A. Mccollam, Y. Matsuda, T. Shibauchi, and A. Carrington, Phys. Rev. Lett. **104**, 057008 (2010).
[35] S. Kasahara, T. Shibauchi, K. Hashimoto, K. Ikada, S. Tonegawa, R. Okazaki, H. Ikeda, H. Takeya, K. Hirata, T. Terashima, and Y. Matsuda, arXiv:0905.4427 (unpublished).
[36] K. Hashimoto, M. Yamashita, S. Kasahara, Y. Senshu, N. Nakata, S. Tonegawa, K. Ikada, A. Serafin, A. Carrington, T. Terashima, H. Ikeda, T. Shibauchi, and Y. Matsuda, arXiv:0907.4399 (unpublished).
[37] K. Machida, J. Phys. Soc. Jpn. **50**, 2195 (1981).
[38] K. Machida and T. Matsubara, J. Phys. Soc. Jpn. **50**, 3231 (1981).
[39] K. Machida and M. Kato, Phys. Rev. Lett. **58**, 1986 (1987); M. Kato and K. Machida, J. Phys. Soc. Jpn. **56**, 2136 (1987); Phys. Rev. B **37**, 1510 (1988).
[40] D. Parker, M. G. Vavilov, A. V. Chubukov, and I. I. Mazin, Phys. Rev. B **80**, 100508(R) (2009).
[41] M. G. Vavilov, A. V. Chubukov, and A. B. Vorontsov, Supercond. Sci. Technol. **23**, 054011 (2010).
[42] A. B. Vorontsov, M. G. Vavilov, and A. V. Chubukov, Phys. Rev. B **79**, 060508(R) (2009).
[43] V. Cvetkovic and Z. Tesanovic, EPL **85**, 37002 (2009).
[44] F. Wang, H. Zhai, Y. Ran, A. Vishwanath, and D. H. Lee, Phys. Rev. Lett. **102**, 047005 (2009).
[45] C. Platt, C. Honerkamp, and W. Hanke, New J. Phys. **11**, 055058 (2009).
[46] S. Raghu, X. L. Qi, C. X. Liu, D. J. Scalapino, and S. C. Zhang, Phys. Rev. B **77**, 220503(R) (2008).
[47] J. Lorenzana, G. Seibold, C. Ortix, and M. Grilli, Phys. Rev. Lett. **101**, 186402 (2008).
[48] P. M. R. Brydon and C. Timm, Phys. Rev. B **79**, 180504(R) (2009).
[49] M. D. Johannes and I. I. Mazin, Phys. Rev. B **79**, 220510(R) (2009).
[50] I. I. Mazin and M. D. Johannes, Nat. Phys. **5**, 141 (2009).
[51] I. Eremin and A. V. Chubukov, Phys. Rev. B **81**, 024511 (2010).
[52] L. Gor'kov and G. Teitel'baum, arXiv:1001.4641 (unpublished).
[53] J. Luttinger and J. Ward, Phys. Rev. **118**, 1417 (1960).
[54] C. DeDominicis and P. Martin, J. Math. Phys. **5**, 14 (1964); **5**, 31 (1964).
[55] D. Rainer and J. W. Serene, Phys. Rev. B **13**, 4745 (1976).
[56] P. Fulde and R. Ferrell, Phys. Rev. **135**, A550 (1964); A. I. Larkin and Y. N. Ovchinnikov, Zh. Eksp. Teor. Fiz. **47**, 1136 (1964) [Sov. Phys. JETP **20**, 762 (1965)].
[57] T. Rice, Phys. Rev. B **2**, 3619 (1970).
[58] N. Kulikov and V. V. Tugushev, Usp. Fiz. Nauk **144**, 643 (1984) [Sov. Phys. Usp. **27**, 954 (1984)].
[59] E. Fawcett, H. L. Alberts, V. Y. Galkin, D. R. Noakes, and J. V. Yakhmi, Rev. Mod. Phys. **66**, 25 (1994).
[60] V. Cvetkovic and Z. Tesanovic, Phys. Rev. B **80**, 024512 (2009).
[61] A. V. Chubukov, A. B. Vorontsov, and M. G. Vavilov (unpublished).
[62] A. A. Abrikosov, *Fundamentals of the Theory of Metals* (Elsevier, New York, 1988).
[63] A *d*-wave symmetry gap presumably lies in between these two cases as some parts of the nested hole and electron FSs will have the gaps of the same sign while other parts will have the opposite signs (Ref. 29).